IEC/TR 62581

Edition 1.0 2010-08

TECHNICAL REPORT

Electrical steel – Methods of measurement of the magnetostriction characteristics by means of single sheet and Epstein test specimens

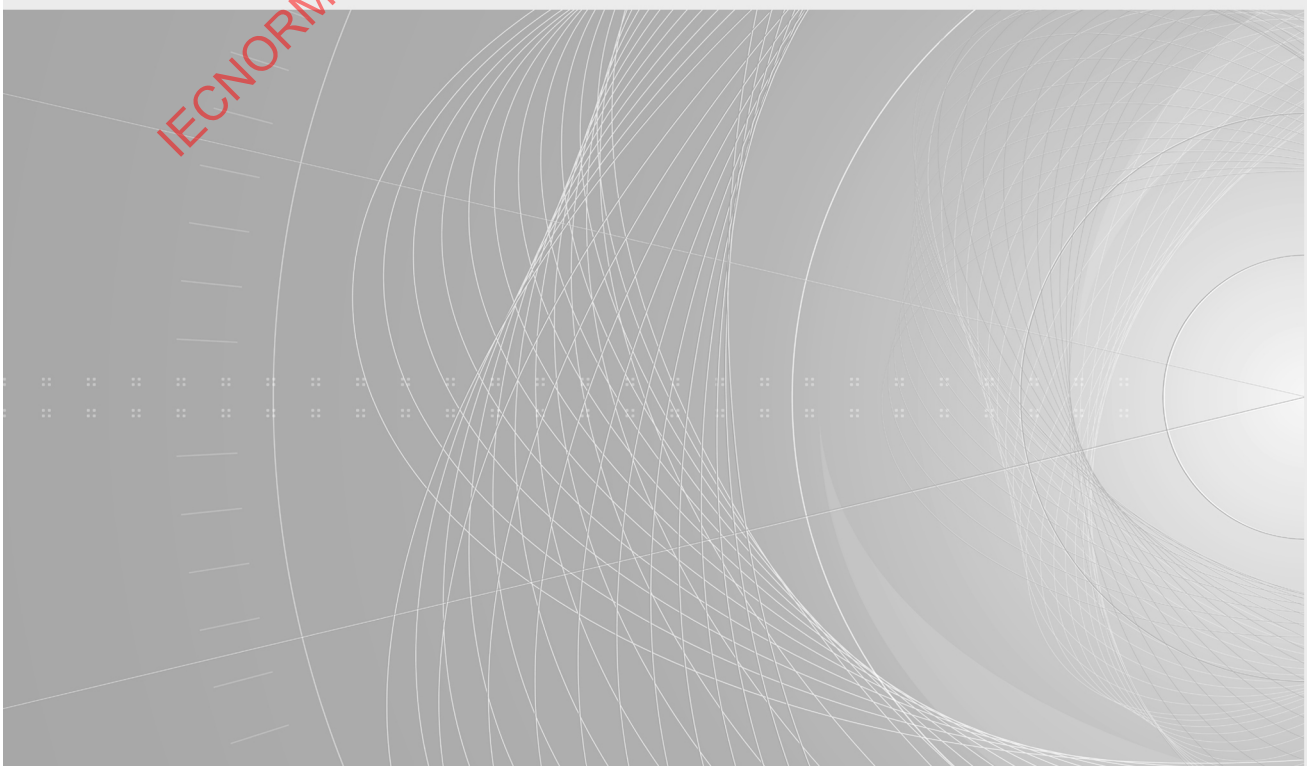

IEC Central Office
3, rue de Varembé
CH-1211 Geneva 20
Switzerland
Email: inmail@iec.ch
Web: www.iec.ch

About IEC publications

The technical content of IEC publications is kept under constant review by the IEC. Please make sure that you have the latest edition, a corrigenda or an amendment might have been published.

- Catalogue of IEC publications: www.iec.ch/searchpub
The IEC on-line Catalogue enables you to search by a variety of criteria (reference number, text, technical committee,…). It also gives information on projects, withdrawn and replaced publications.

- IEC Just Published: www.iec.ch/online_news/justpub
Stay up to date on all new IEC publications. Just Published details twice a month all new publications released. Available on-line and also by email.

- Electropedia: www.electropedia.org
The world's leading online dictionary of electronic and electrical terms containing more than 20 000 terms and definitions in English and French, with equivalent terms in additional languages. Also known as the International Electrotechnical Vocabulary online.

- Customer Service Centre: www.iec.ch/webstore/custserv
If you wish to give us your feedback on this publication or need further assistance, please visit the Customer Service Centre FAQ or contact us:

Email: csc@iec.ch
Tel.: +41 22 919 02 11
Fax: +41 22 919 03 00

IEC/TR 62581

Edition 1.0 2010-08

TECHNICAL REPORT

Electrical steel – Methods of measurement of the magnetostriction characteristics by means of single sheet and Epstein test specimens

INTERNATIONAL ELECTROTECHNICAL COMMISSION

PRICE CODE X

ICS 29.030

ISBN 978-2-88912-101-4

CONTENTS

INTERNATIONAL ELECTROTECHNICAL COMMISSION

ELECTRICAL STEEL – METHODS OF MEASUREMENT OF THE MAGNETOSTRICTION CHARACTERISTICS BY MEANS OF SINGLE SHEET AND EPSTEIN TEST SPECIMENS

FOREWORD

1) The International Electrotechnical Commission (IEC) is a worldwide organization for standardization comprising all national electrotechnical committees (IEC National Committees). The object of IEC is to promote international co-operation on all questions concerning standardization in the electrical and electronic fields. To this end and in addition to other activities, IEC publishes International Standards, Technical Specifications, Technical Reports, Publicly Available Specifications (PAS) and Guides (hereafter referred to as "IEC Publication(s)"). Their preparation is entrusted to technical committees; any IEC National Committee interested in the subject dealt with may participate in this preparatory work. International, governmental and non-governmental organizations liaising with the IEC also participate in this preparation. IEC collaborates closely with the International Organization for Standardization (ISO) in accordance with conditions determined by agreement between the two organizations.
2) The formal decisions or agreements of IEC on technical matters express, as nearly as possible, an international consensus of opinion on the relevant subjects since each technical committee has representation from all interested IEC National Committees.
3) IEC Publications have the form of recommendations for international use and are accepted by IEC National Committees in that sense. While all reasonable efforts are made to ensure that the technical content of IEC Publications is accurate, IEC cannot be held responsible for the way in which they are used or for any misinterpretation by any end user.
4) In order to promote international uniformity, IEC National Committees undertake to apply IEC Publications transparently to the maximum extent possible in their national and regional publications. Any divergence between any IEC Publication and the corresponding national or regional publication shall be clearly indicated in the latter.
5) IEC itself does not provide any attestation of conformity. Independent certification bodies provide conformity assessment services and, in some areas, access to IEC marks of conformity. IEC is not responsible for any services carried out by independent certification bodies.
6) All users should ensure that they have the latest edition of this publication.
7) No liability shall attach to IEC or its directors, employees, servants or agents including individual experts and members of its technical committees and IEC National Committees for any personal injury, property damage or other damage of any nature whatsoever, whether direct or indirect, or for costs (including legal fees) and expenses arising out of the publication, use of, or reliance upon, this IEC Publication or any other IEC Publications.
8) Attention is drawn to the Normative references cited in this publication. Use of the referenced publications is indispensable for the correct application of this publication.
9) Attention is drawn to the possibility that some of the elements of this IEC Publication may be the subject of patent rights. IEC shall not be held responsible for identifying any or all such patent rights.

The main task of IEC technical committees is to prepare International Standards. However, a technical committee may propose the publication of a technical report when it has collected data of a different kind from that which is normally published as an International Standard, for example "state of the art".

IEC 62581, which is a technical report, has been prepared by IEC technical committee 68: Magnetic alloys and steels.

The text of this technical report is based on the following documents:

Enquiry draft	Report on voting
68/411/DTR	68/414/RVC

Full information on the voting for the approval of this technical report can be found in the report on voting indicated in the above table.

This publication has been drafted in accordance with the ISO/IEC Directives, Part 2.

The committee has decided that the contents of this publication will remain unchanged until the stability date indicated on the IEC web site under "http://webstore.iec.ch" in the data related to the specific publication. At this date, the publication will be

- reconfirmed,
- withdrawn,
- replaced by a revised edition, or
- amended.

A bilingual version of this publication may be issued at a later date.

INTRODUCTION

Magnetostriction is one of the magnetic properties that accompany ferromagnetism. It causes reversible deformations of a material body due to magnetization arising from an applied magnetic field.

Nowadays, the environmental problem of acoustic noise pollution caused by transformers and other applications of electrical steels (e.g. ballast, motors, etc.) is a concern of industry [31][1]. Magnetostriction of electrical steels is recognized as one of the causes of the problem and a standardization of methods of measurement of the magnetostriction is required to advance developments in materials to address this problem.

Historically, several methods have been used to measure magnetostriction including strain gauge, capacitance, differential transformer, piezoelectric pick-up and piezoelectric accelerometer methods. However, these methods require skill to set up the sensor accurately and to avoid vibrational noise that accompanies these contact methods. To solve these problems, optical methods that adopt optical vibrometers and optical displacement meters have been developed [1]-[8].

The optical method satisfies the following requirements for the measurement: non-contact, high resolution, high reproducibility and ease of operation without any special skill on the part of the operator. Several optical sensors can be used: laser Doppler vibrometers, heterodyne displacement meters and laser displacement meters with high resolution.

Magnetostriction is a magneto-mechanical phenomenon which accompanies the change of the volume fraction of magnetic domains which have a certain magnetic orientation with respect to the direction of the applied magnetic field, and which is intrinsically sensitive to stress [14],[15]. The stress sensitivity is dependent on material conditions such as grain orientation, residual stress and coating tension. The magnetostriction of electrical steel is increased by compressive stresses in the magnetizing direction rather than tensile stresses [9],[16]-[23]. Magnetic cores of electrical machines such as transformers often contain areas of increased stress. Therefore the stress sensitivity should be evaluated under a specified stress.

The acoustic noise emission from transformers and other machines is usually evaluated in terms of the A-weighted sound pressure level specified in IEC 61672-1. Vibration velocities caused by magnetostriction are transformed into sound pressure on the surface of the materials. Therefore, A-weighted characteristics of magnetostriction, such as A-weighted magnetostriction velocity level or A-weighted magnetostriction acceleration level, are necessary for the assessment of electrical steel sheets with respect to the acoustic noise [24]-[26].

This technical report is comprised of articles which review the optical and accelerometer methods of measurement of magnetostriction with the aim of producing a standard method of measurement of magnetostriction.

Two methods, by a single sheet tester and by a single strip tester, are described. The former should be applied to single sheet specimens with width of not less than 100 mm which have not been stress relief annealed. The latter method should be applied to Epstein test specimens, which may have been stress relief annealed to remove stresses imparted to the specimens during preparation.

---

1 The figures in square brackets refer to the Bibliography.

ELECTRICAL STEEL – METHODS OF MEASUREMENT OF THE MAGNETOSTRICTION CHARACTERISTICS BY MEANS OF SINGLE SHEET AND EPSTEIN TEST SPECIMENS

1 Scope

This technical report describes the general principles and technical details of the measurement of the magnetostriction of single sheet specimens preferably 500 mm long and 100 mm wide and Epstein strip specimens, specified in IEC 60404-2, of electrical steel by means of optical sensors and accelerometers.

These methods are applicable to test specimens obtained from electrical steel sheets and strips of any grade. The characteristics of magnetostriction are determined for a sinusoidal induced voltage, for specified peak values of magnetic polarization and for a specified frequency.

The measurements are made at an ambient temperature of 23 °C ± 5 °C on test specimens which have first been demagnetized.

2 Normative references

The following referenced documents are indispensable for the application of this document. For dated references, only the edition cited applies. For undated references, the latest edition of the referenced document (including any amendments) applies.

IEC 60050-121, *International Electrotechnical Vocabulary – Part 121: Electromagnetism*

IEC 60050-221, *International Electrotechnical Vocabulary – Chapter 221: Magnetic materials and components*

IEC 60404-2, *Magnetic materials – Part 2: Methods of measurement of the magnetic properties of electrical steel sheet and strip by means of an Epstein frame*

IEC 60404-3:1992, *Magnetic materials – Part 3: Methods of measurement of the magnetic properties of electrical steel strip and sheet by means of a single sheet tester*
Amendment 1 (2002)
Amendment 2 (2009)

IEC 61672-1, *Electroacoustics – Sound level meters – Part 1: Specifications*

3 Terms and definitions

For the purpose of this document, the definitions of the principal terms relating to magnetic properties given in IEC 60050-121 and IEC 60050-221 apply, as well as the following terms and definitions:

3.1
butterfly loop
hysteresis loop of the strain measured in the direction of applied field versus the magnetic polarization for a period of an alternating magnetization

3.2
zero-to-peak magnetostriction
λ_{o-p}
net strain measured in the direction of applied field from the zero magnetic polarization to a given magnetic polarization

3.3
peak-to-peak magnetostriction
λ_{p-p}
amplitude of the strain measured in the direction of the applied field under alternating magnetization

4 Method of measurement of the magnetostriction characteristics of electrical steel sheets under applied stress by means of a single sheet tester

4.1 Principle of the method

Measurement systems for magnetostriction are shown in Figure 1 and Figure 2. A block diagram of the measurement system is shown in Figure 3.

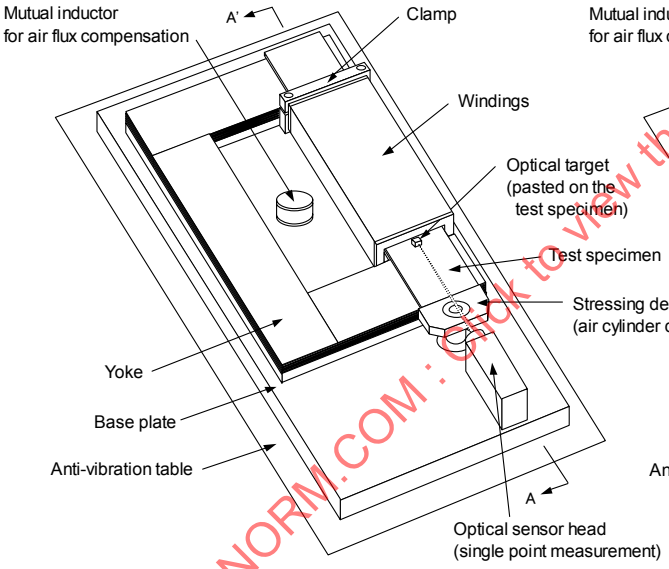

Figure 1a – Single point measurement

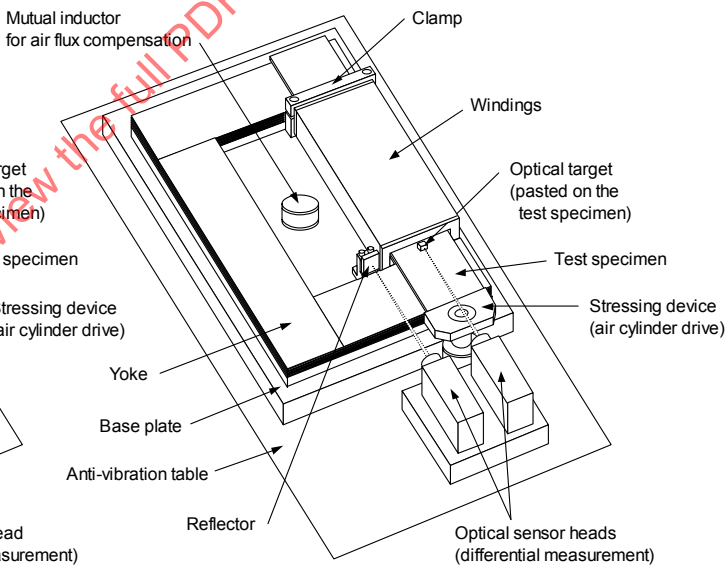

Figure 1b – Differential measurement

Figure 1 – Measurement systems for magnetostriction

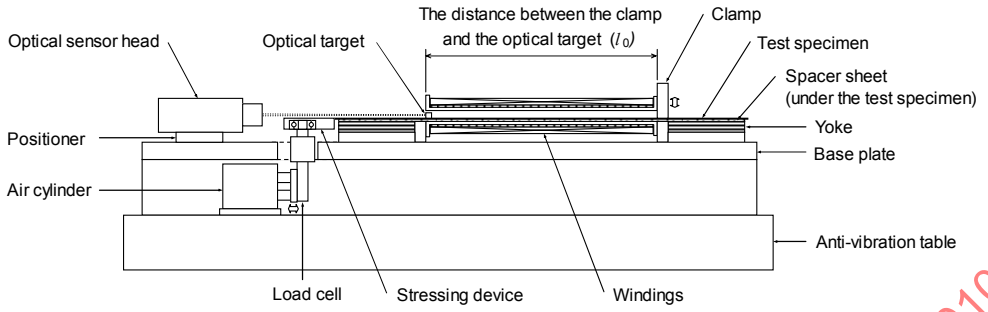

Figure 2 – Section of the test frame; A-A' in Figure 1

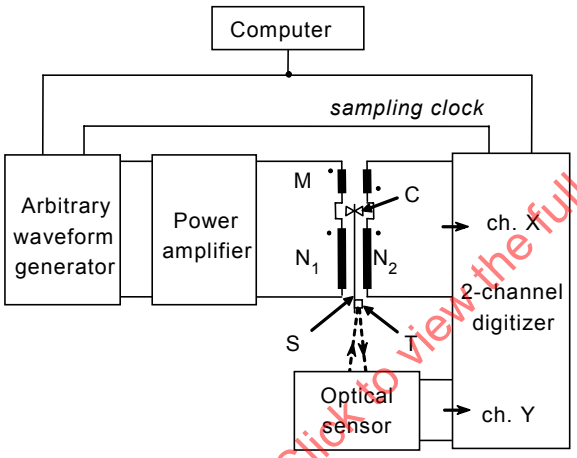

S test specimen
T optical target
C clamp
M mutual inductor for air flux compensation
N_1 primary winding
N_2 secondary winding

Figure 3 – Block diagram of the measurement system

The test specimen comprises a sample of electrical steel sheet and is placed inside two windings:

– an external primary winding;

– an interior secondary winding.

The flux closure is made by a magnetic circuit consisting of a yoke, the cross-section of which is large compared with that of the test specimen. There are narrow and homogeneous gaps between the test specimen and the pole faces of the yoke to weaken the electromagnetic force between them. The test frame that consists of the yoke, the windings and a clamp should be permanently fixed to a rigid base during the measurement.

The test specimen is fixed to the base at one end of the windings using the clamp shown in Figure 1. An optical target is pasted on the centerline of the surface of the test specimen at the other end of the windings. Changes in length between the clamping point and the optical target are measured using an optical sensor.

In order to reduce the effect of stray fields between the test specimen and the pole faces, the optical sensor should be at a sufficient working distance from the test frame.

Two measurement types of optical sensor can be used: a single point measurement and a differential measurement. The single point measurement uses a sensor head fixed on the base and measures vibration or displacement between the optical target and the sensor head. The differential measurement uses two sensor heads and measures vibration and displacement between the optical target and a reflector fixed on the base. The latter system has advantages of (a) cancellation of external noise and in (b) setting the sensors separately from the base.

Care shall be taken to minimize noise vibrations caused by resonances of the test frame and external vibrations. The test frame shall be placed on an anti-vibration table in order to isolate the test frame from external vibration.

Care shall be taken to prevent out-of-plane deformations of the test specimen. The test specimen shall be placed on a flat and smooth surface in the test frame and kept flat during the measurement (see Annex A).

4.2 Test specimen

The length of the test specimen should be not less than 500 mm. The part of the specimen situated outside the pole faces should not be longer than is necessary to facilitate insertion and removal of the test specimen and to apply an external stress to the test specimen in the longitudinal direction.

The width of the test specimen should be not less than 100 mm.

NOTE Since the average grain diameter for the high permeability grain-oriented electrical steel sheet is about 10-20 mm, a comparatively large sample size is required. The test specimen should be wide enough to take into account the affected region close to the cut edges. However, it may be difficult to produce a flux closure yoke with flat and coplanar faces for wider test specimens.

The test specimen should be cut without forming large burrs or mechanical distortion. The test specimen shall be flat. When a test specimen is cut, the edge of the parent strip is taken as the reference direction. The following tolerances are allowed for in the angle between the direction of rolling and that of cutting:

– ±1° for grain-oriented electrical steel sheet;

– ±5° for non-oriented electrical steel sheet.

4.3 Yokes

Several types of yoke can be used (see Figure 4):

– a horizontal single or double yoke;

– a vertical single or double yoke.

The horizontal yokes make a horizontal flux closure and the vertical yokes make a vertical flux closure. Each pole face is horizontal in both types of yoke.

Each yoke is made up of insulated sheets of grain-oriented electrical steel or nickel iron alloy. It should have a low reluctance and therefore stress relief annealing of the cut strips is required. The two pole faces of each yoke shall be coplanar within 0,03 mm (see Annex A). The yokes shall be constructed in accordance with the requirements of Annex A of IEC 60404-8.

In order to reduce the effect of eddy currents and give a more homogeneous distribution of the flux over the inside of the yokes, the yokes are made of a glued stack of laminations or C-cores. In the former case the corners have staggered butt joints. The overlap length of the test specimen and the pole faces shall be long enough and not less than 25 mm.

Before use, the yokes should be carefully demagnetized.

The electromagnetic force between the test specimen and the pole faces should be reduced by inserting narrow and uniform gaps between them. This can be achieved by inserting a sheet under the test specimen. The sheet shall be made of a non-compressible, non-conducting and non-magnetic material with flat and smooth surfaces. The thickness of the sheet should be uniform and between 0,1 mm and 1,0 mm.

NOTE 1 The electromagnetic force may increase out-of-plane vibrations of the test specimen and friction between the test specimen and the pole faces. These may reduce the accuracy and reproducibility of the measurement.

Each yoke is glued to the base plate. Resonances in each yoke that may affect the measurement shall be avoided.

In the case of the vertical double yoke, care should be taken to maintain a constant gap between the test specimen and the pole faces of the upper yoke.

NOTE 2 Because the upper yoke may block the optical beam from the sensor heads, the optical target may be outside the upper yoke in this case. Over the pole face region there will be perpendicular components of the magnetic flux in the test specimen and therefore over this region the magnetostriction behaviour may change. Verification of test results with the other test frame may be necessary.

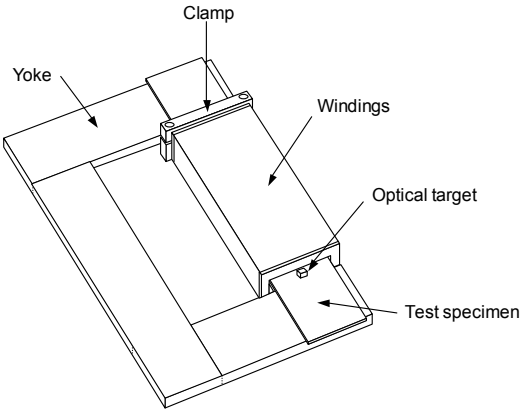

Figure 4a – Horizontal single yoke

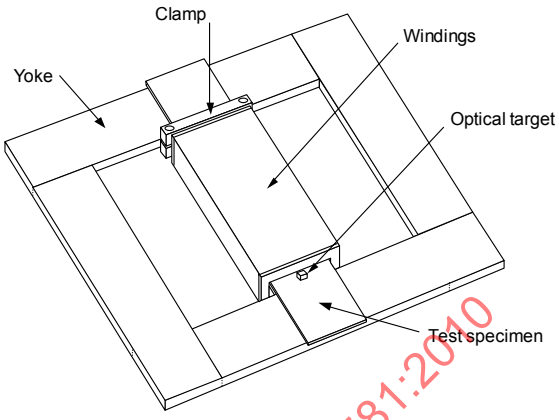

Figure 4b – Horizontal double yoke

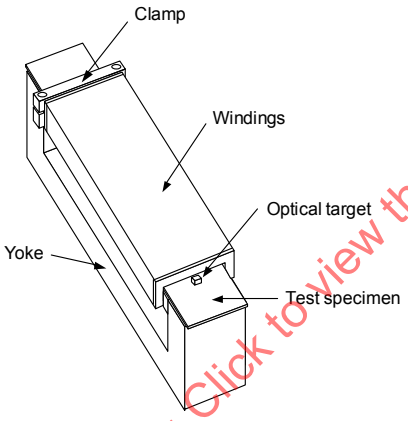

Figure 4c – Vertical single yoke

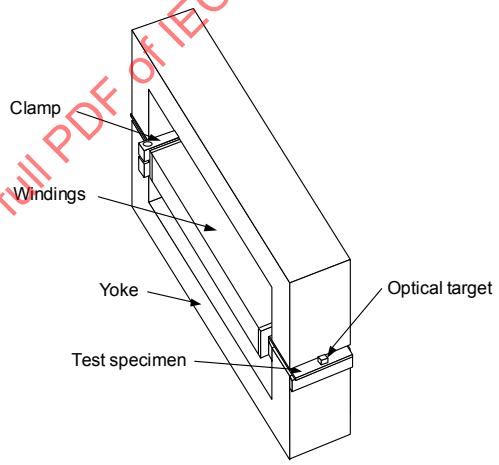

Figure 4d – Vertical double yoke

Figure 4 – Frames with various types of yoke

4.4 Windings

The primary and secondary windings are wound on a rectangular former made of non-conducting, non-magnetic material. The length of the former is shorter than the distance between the pole faces of the yokes to avoid the effect of stray fields between the test specimen and the pole faces.

The number of turns of the primary winding will depend on the characteristics of the power supply.

The number of turns of the secondary winding will depend on the characteristics of the measuring instruments.

The test specimen is inserted through the inside hollow of the former and supported on a plate of non-conducting and non-magnetic material. The surface of the plate in contact with the test specimen shall be flat and smooth with its surface coplanar with the pole faces within 0,03 mm (see Annex A).

4.5 Air flux compensation

Compensation should be made for the effect of air flux, for example, by means of a mutual inductor.

The primary winding of the mutual inductor is connected in series with the primary winding of the test frame, while the secondary winding of the mutual inductor is connected to the secondary winding of the test frame in series opposition.

The adjustment of the mutual inductance shall be made so that, when passing an alternating current through the primary winding in the absence of the specimen in the test frame, the voltage measured between the non-common terminals of the secondary windings should be no more than 0,1 % of the voltage appearing across the secondary winding of the test frame alone.

Thus the average value of the rectified voltage induced in the combined secondary windings is proportional to the peak value of the magnetic polarization in the test specimen.

Compensation can be achieved by a digital method without the mutual inductor. The contribution of air flux in the secondary induced voltage can be calculated from the primary current and then by subtracting it from the measured secondary induced voltage.

4.6 Power supply

The power supply should be of low internal impedance and should be highly stable in terms of voltage and frequency. During the measurement, the voltage and the frequency should be maintained constant within ± 0,2 %.

The power supply comprises an arbitrary signal generator consisting of a waveform synthesizer and voltage and frequency controller and a power amplifier. The arbitrary signal generator shall have two outputs: one for the magnetizing signal supplied to the power amplifier and the other for the synchronized sampling clock supplied to a 2-channel digitizer.

In addition, the waveform of the secondary induced voltage should be maintained as near sinusoidal as possible. It is preferable to maintain the form factor of the secondary voltage to within ± 1 % of 1,111. This can be achieved by various means, for example, by using an electronic feedback amplifier or by a digital feedback procedure through a computer.

4.7 Optical sensor

The optical sensor can detect changes in displacement of the optical target fixed on the test specimen with a high resolution of better than 10 nm in the displacement of the optical target at the frequency of 100 Hz. However, a resolution of better than 3 nm is recommended.

NOTE The resolution of the length of 10 nm corresponds to a resolution of $3{,}3 \times 10^{-8}$ in magnetostriction for a distance of 300 mm between the clamp and the optical target. The higher resolution of 1×10^{-8} in magnetostriction is required for high permeability grain-oriented electrical steel sheet used for low noise transformers in which the magnetostriction is less than 1×10^{-6}.

Either optical vibrometer or optical displacement meters can be used. The optical vibrometer, e.g. a laser Doppler vibrometer, detects changes in displacement of the optical target and is suitable for a.c. measurements. The optical displacement meter, e.g. a heterodyne displacement meter, detects the displacement of the optical target from the sensor head and is suitable for d.c. measurements and a.c. measurements at low frequency.

A laser Doppler vibrometer is recommended for the optical vibrometer. This sensor has adequate performance for measurements of the magnetostriction: high spatial resolution, high stability, a wide range of frequency and velocity, and is unaffected by magnetic field and temperature. It may be used remotely to enable flexibility in sensor positioning. It is readily available and requires little operator skill.

Two measurement methods are available for optical sensors: a single point measurement method and a differential measurement method. The single point measurement method adopts a sensor head and measures vibration or displacement between the optical target and the sensor head. The differential measurement method adopts two sensor heads and measures the difference of vibration or displacement between the optical target on the test specimen and the reflector fixed on the test frame base. The differential measurement method has the advantage that the sensor heads are divorced from the test frame base and any external noise is cancelled and therefore is not detected.

In the case of optical sensors, beams of light are focused on the optical target or the reflector. The optical target and the reflector reflect back the beams of light to the optical sensor. The optical target should be of low profile, low mass (less than 0,05 g) and made of a non-conducting and non-magnetic material in order to undertake measurements of magnetostriction: for example, 4 mm in height and 3 mm to 5 mm in width and depth. The optical target can be pasted at a fixed position on the test specimen before inserting the test specimen into the test frame. Reflecting thin films can be pasted on the surfaces of the optical target and the reflector facing the optical sensors.

4.8 Stressing device

The stressing device should apply the stress along the axis of the test specimen. An air cylinder, which is fastened to the base plate, holds the stressing device and drives the stressing device in the direction of the axis of the test specimen. Another device can be used instead of the air cylinder if it is flexible to length change of the test specimen caused by magnetostriction. A load cell is installed between the stressing device and the air cylinder to detect stresses applied to the test specimen. These devices shall be prepared so as not to prevent the magnetostriction measurement by those resonances.

The stressing device applies compressive stress to the test specimen when the magnetostriction under compressive stress is measured, otherwise the stressing device shall be retracted and removed from the test specimen. Stresses of up to 5 MPa can be applied between the clamp and the stressing device in the longitudinal direction of the test specimen. A low friction, non-rotating air cylinder can be used for this purpose (see Figure 2).

NOTE The stress sensitivity of magnetostriction may be measured at a specified compressive stress of, for example, 3 MPa.

The pressure of the air cylinder can be controlled easily by air through an electro-pneumatic valve controlled by a d.c. voltage. The load cell installed between the test specimen and the air cylinder detects the stress.

4.9 Data acquisitions

The output voltage of the optical sensor and the secondary induced voltage shall be digitized simultaneously and recorded as a set of signal data by a 2-channel digitizer.

NOTE A 2-channel digital sampling oscilloscope can be used as the 2-channel digitizer.

The 2-channel digitizer has two independent channels composed of calibrated amplifiers, sample-and-hold circuits and calibrated analogue to digital converters (ADC). The gain selectable amplifiers should enable a wide range of input voltage and frequency. The 2-channels are sampled simultaneously with the sampling clock generated by the arbitrary signal generator and then digitized. The resolution of ADC shall be a minimum of 12 bits.

To avoid loading the secondary winding, the 2-channel digitizer should have sufficiently high input impedance and low capacitance (typically 1 MΩ in parallel with about 100 pF).

The output voltage of the laser Doppler vibrometer is proportional to the time derivative of magnetostriction $\mathrm{d}\lambda(t)/\mathrm{d}t$. On the other hand, the output of the heterodyne displacement meter is proportional to the magnetostriction $\lambda(t)$.

The secondary induced voltage is proportion to the time derivative of magnetic polarization $\mathrm{d}J(t)/\mathrm{d}t$. Two approaches can be used for the integration of derivative signals to obtain $\lambda(t)$ from $\mathrm{d}\lambda(t)/\mathrm{d}t$ and $J(t)$ from $\mathrm{d}J(t)/\mathrm{d}t$:

– analogue integration and digitizing;
– digitizing and numerical integration.

The former approach requires analogue integrators with wide input voltage and frequency ranges. The latter approach requires ADC with the wide input ranges and higher resolutions.

It is recommended that the sampling frequency is a multiple of the magnetizing frequency (Nyquist condition) and sufficiently large to reduce a digitizing error. It is convenient that the number of samples per period of magnetization shall be equal to the power of 2 in terms of digital data processing such as a fast Fourier transform (FFT): for instance 512 or 1024 samples per period of magnetization.

In order to improve data qualities, the data acquisitions can be extended for multiple periods of magnetization and the data are then averaged into periodical signal data.

4.10 Data processing

The signal data which has been obtained are processed numerically by computer by

– integration;
– fast Fourier transform (FFT);
– reconstruction of signals after band pass filtering;
– calculation of the A-weighted magnetostriction characteristics (see Annex C).

4.11 Preparation for measurement

The length of the test specimen should be measured with an accuracy of ± 0,1 % and its mass determined within ± 0,1 %. The test specimen on which the optical target was pasted beforehand shall be loaded and centered on the longitudinal and transverse axes of the windings.

The test specimen should be fastened to the base by the clamp so that the distance between the clamp and the optical target is kept to a set length with an accuracy of ± 0,1 %.

In order to prevent out-of-plane deformations of the test specimen, a thin glass plate or a slight load may be placed on the test specimen. The load should not be so excessive as to bring about deformations of the test specimen caused by magnetostriction.

In the case of measurement under applied stress, compressive stress is slowly applied to the test specimen, using the stressing device, until the load indicator has reached the required value. Care should be taken to avoid an excessive load and out-of-plane deformations of the test specimen.

In the case of the vertical double yoke frame, the partly counterbalanced upper yoke is lowered.

Before the measurement, the test specimen should be demagnetized by slowly decreasing an alternating magnetic field starting from well above the value to be measured.

The output voltage of the optical sensor and the secondary induced voltage are digitized by the 2-channel digitizer. If the analogue integration is adopted, the output voltage of the analogue integrator shall be digitized instead.

4.12 Adjustment of power supply

The power supply output is slowly increased until the desired peak value of magnetic polarization $\hat{J}$ is reached.

The peak value of magnetic polarization can be determined by digitized data of the secondary induced voltage.

An alternative method of the adjustment is possible. An average type voltmeter with sufficiently high input impedance and low capacitance (typically 1 MΩ in parallel with about 100 pF) can be connected to the input terminal of the 2-channel digitizer. The power supply output should be slowly increased until the average rectified value of the secondary voltage $\overline{|U_2|}$ has reached the required value. This is calculated from the desired peak value of magnetic polarization $\hat{J}$ by means of

$$\overline{|U_2|} = 4 f N_2 A \hat{J} \tag{1}$$

where

$\overline{|U_2|}$ is the average value of the secondary rectified voltage, in volts;

f is the frequency, in hertz;

N_2 is the number of turns of the secondary winding;

A is the cross-sectional area of the test specimen, in square metres;

$\hat{J}$ is the peak value of magnetic polarization, in tesla.

The cross-sectional area A is given by the equation

$$A = \frac{m}{l \rho_{\mathrm{m}}} \tag{2}$$

where

m is the mass of the test specimen, in kilograms;

l is the length of the test specimen, in metres;

ρ_{m} is the density of the test material, in kilograms per cubic metre.

4.13 Measurement

The instantaneous value of the magnetostriction $\lambda(t)$ is measured by the change in a base length l_0 within the uniformly magnetized area of the test specimen:

$$\lambda(t) = \frac{\Delta l_0(t)}{l_0} \tag{3}$$

where

$\lambda(t)$ is the instantaneous value of the magnetostriction at time t;

$\Delta l_0(t)$ is the change in the base length at time t from the length in demagnetized state, in metres;

l_0 is the base length of the test specimen, in metres.

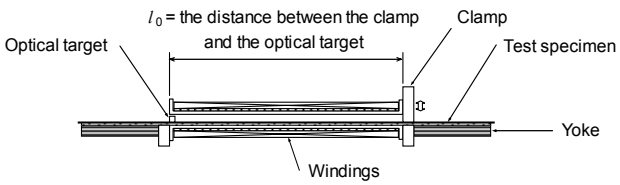

Figure 5a – Horizontal single or double yoke type and Vertical single yoke type

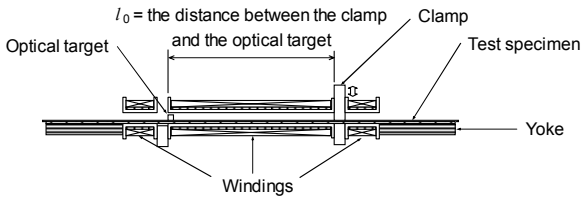

Figure 5b – Split winding type of Figure 5a (see Figure 9)

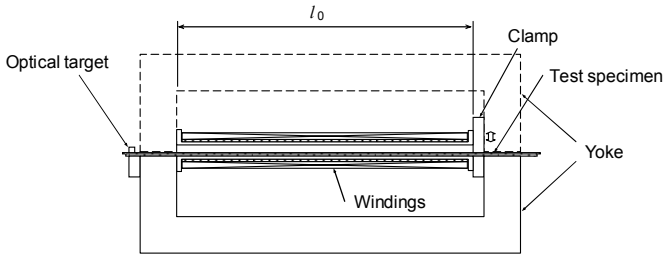

Figure 5c – Vertical single or double yoke

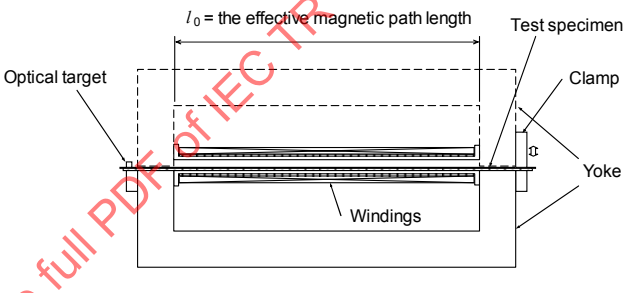

Figure 5d – Vertical single or double yoke type; different arrangement from Figure 5c

Figure 5 – Base length l_0 for various types of frame (see Figure 4)

Figure 5 shows the base length l_0 for various types of frame shown in Figure 4. In the case that the clamp and the optical target are arranged at the inside of yoke, the base length is the distance between the clamp and the optical target on the test specimen. In the other case, the base distance is shorter than the distance between the clamp and the optical target. The part of the test specimen close to the inner part of the yoke may show higher magnetostriction than the rest of the test specimen due to increases in 90° domain volumes (see 7.1) by magnetic flux shorting to the yoke. Therefore a careful calibration of the base length is necessary in the latter case.

The data acquisitions are executed for multiple periods of magnetization by the 2-channel digitizer and the data are averaged into periodical signal data.

The output voltage of the laser Doppler vibrometer U_v is proportional to the time derivative of length change of the test specimen:

$$U_\mathrm{v} = k_\mathrm{v}\, l_0\, \frac{\mathrm{d}\lambda(t)}{\mathrm{d}t} \tag{4}$$

where

U_v is the output voltage of the laser Doppler vibrometer, in volts;

k_v is the sensitivity of the laser Doppler vibrometer, in volts second per metre;

l_0 is the base length on the test specimen, in metres;

$\lambda(t)$ is the instantaneous value of the magnetostriction at time t.

The secondary induced voltage U_2 is in proportion to the time derivative of magnetic polarization:

$$U_2 = -N_2 A \frac{\mathrm{d}J(t)}{\mathrm{d}t} \tag{5}$$

where

U_2 is the secondary induced voltage, in volts;

N_2 is the number of turns of the secondary winding;

A is the cross-sectional area of the test specimen, in square metres;

$J(t)$ is the instantaneous value of the magnetic polarization at time, t, in tesla.

The magnetostriction $\lambda(t)$ and magnetic polarization $J(t)$ can be obtained by integration of equations (4) and (5):

$$\lambda(t) = \frac{1}{k_\mathrm{v} l_\mathrm{m}} \int U_\mathrm{v} \,\mathrm{d}t + C_\mathrm{v} \tag{6}$$

$$J(t) = -\frac{1}{N_2 A} \int U_2 \,\mathrm{d}t + C_2 \tag{7}$$

where

C_v is the integration constant which can be determined from the following relation:

$$\lambda(t) = 0 \text{ at } J(t) = 0 \tag{8}$$

C_2 is the integration constant which can be determined from the following relation:

$$\int_0^{1/f} J(t) \,\mathrm{d}t = 0 \tag{9}$$

When analogue integrators are not adopted, the integrations in equations (6) and (7) are executed through the data processing in the computer. Alternatively, these integrations are executed by the analogue integrators.

In the case where the heterodyne displacement meter is adopted instead of the laser Doppler vibrometer, the following equation is to be used instead of equation (6):

$$\lambda(t) = \frac{1}{k_\mathrm{d} l_\mathrm{m}} U_\mathrm{d} \tag{10}$$

where

U_d is the output voltage of the heterodyne displacement meter, in volts;

k_d is the sensitivity of the heterodyne displacement meter, in volts per metre;

l_m is the distance between the clamp and the optical target on the test specimen, in metres.

If the signal to noise ratio of the magnetostriction $\lambda(t)$ and the magnetic polarization $J(t)$ are not sufficiently high, they may be increased through digital band pass filtering in the numerical mode.

As the odd harmonic components of magnetostriction do not exist theoretically under sinusoidal magnetization, they could be eliminated as noise. If the sampling number per magnetic period is even, averaging over a half period could eliminate the odd harmonics component.

4.14 Determination of the butterfly loop

By plotting the magnetostriction $\lambda(t)$ on the vertical axis and the magnetic polarization $J(t)$ on the horizontal axis for a period of magnetization, the butterfly loop can be determined. Figure 6 shows an example of the butterfly loop.

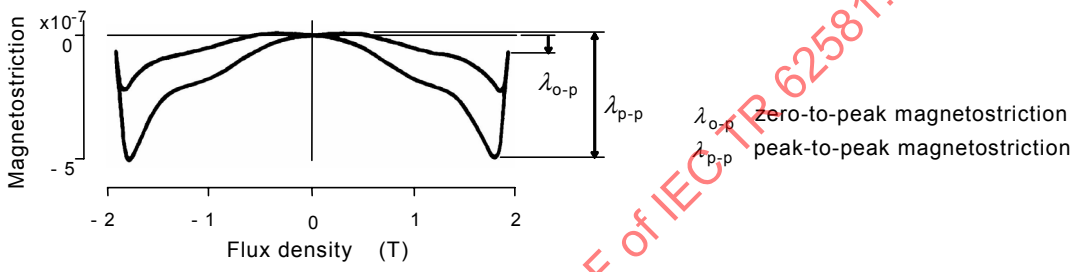

Figure 6 – Butterfly loop and determinations of zero-to-peak and peak-to-peak values of magnetostriction

4.15 Determinations of the zero-to-peak and peak-to-peak values

Figure 6 shows the relationships between a butterfly loop and zero-to-peak and peak-to-peak values of magnetostriction.

The zero-to-peak magnetostriction λ_{o-p} is determined as the instantaneous value of the magnetostriction $\lambda(t)$ at the instant of the maximum magnetic polarization.

The peak-to-peak magnetostriction λ_{p-p} is determined as the amplitude of the magnetostriction $\lambda(t)$ in a period of magnetization.

NOTE For magnetostriction characteristics consider the acoustic A weighting filter; see Annex C.

4.16 Reproducibility

The reproducibility depends on the stress condition of the test specimen in the test frame. The reproducibility of this method, using the test apparatus defined above, is characterized by a relative standard deviation of 5 % for electrical steel sheets.

5 Examples of the measurement systems

5.1 Single sheet tester

Historically, several methods have been used to measure the magnetostriction of electrical steel sheets: strain gauge, capacitance, differential transformer, piezoelectric pick-up and piezoelectric accelerometer methods. However, these methods have difficulties in measurement. The strain gauge method is a local measurement at the point where the gauge is adhered to the test specimen and many gauges are necessary to obtain average characteristics

of magnetostriction over a considerably large area of specimen, especially for high permeability grain-oriented electrical steel sheet with large crystalline grains. The capacitance methods require skill to set up the sensor accurately. The other methods require skill to avoid vibrational noise caused by transmission from equipment in contact with the test specimen.

To solve these problems, non-contact methods using optical sensors have been developed [1]-[9], [11], [15]. Michelson interferometers have been used to detect magnetostriction. Figure 7 shows a measurement system using a Michelson interferometer [1]. The test specimen has a length of 500 mm and a width between 25 mm and 100 mm. An open magnetic circuit is adopted so as to make the test specimen free from any external forces. Two mirrors are pasted to the uniform magnetization part of the test specimen with a separation of 200 mm. Those mirrors constitute parts of the Michelson interferometer. Magnetostriction is detected by the displacement of interference fringes on the screen. The separation distance between the mirrors is measured. The theoretical sensitivity of magnetostriction is 2×10^{-9}.

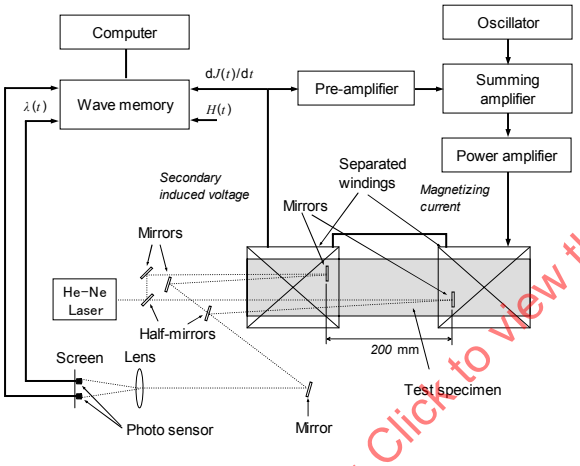

Figure 7 – Measurement system using a Michelson interferometer; differential measurement [1]

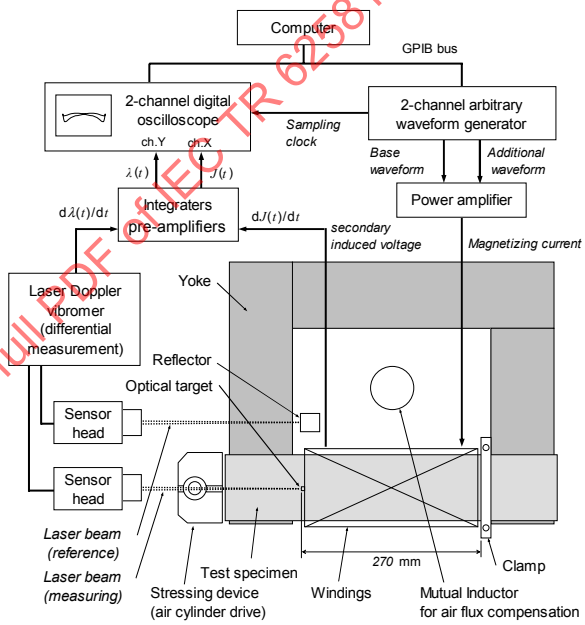

Figure 8 – Measurement system using a laser Doppler vibrometer; differential measurement [2], [3], [17]

The laser Doppler vibrometers have adequate performance for the sensor to detect magnetostriction. They have high spatial resolution, high stability, a wide range of operating frequency and velocity, and are unaffected by magnetic field and temperature. They can work remotely which allows flexibility in the positioning of the sensor and they are readily available, requiring little operator skill. Figure 8 shows a measurement system using a laser Doppler vibrometer to detect magnetostriction velocity [2], [3], [17], [25]. The test specimen has a length of 500 mm and a width of 100 mm. A closed magnetic circuit is formed using a horizontal single yoke [28], [29]. The test specimen is clamped to the base plate at one end of the windings and an optical target is pasted on the test specimen at the other end of the windings. The distance between the clamp and the optical target is 270 mm. The sensor is of the differential measurement type and detects the difference in velocity between the optical target and a reflector fixed on the base plate. The stress sensitivity of magnetostriction can be evaluated using a stressing device driven by an air cylinder and an electro-pneumatic valve controlled by a d.c. voltage. Equipments are digitalized to enable full automatic measurements by computer controls. This system can measure the magnetostriction over the frequency range of 20 Hz to 1000 Hz and under non-sinusoidal magnetization as well as sinusoidal magnetization.

Figure 9 shows a measurement system that uses two different types of sensors: a laser Doppler vibrometer to detect the magnetostriction velocity and a heterodyne displacement meter to detect the magnetostriction [4], [5]. The test specimen has a length of 500 mm and a width of 100 mm. A closed magnetic circuit is formed using a horizontal double yoke. The test specimen is not fixed to the base plate. Two optical targets are fixed on the test specimen with a separation of 170 mm. In the case of the laser Doppler vibrometer, the sensor is a single point measurement type and measurements are repeated for two optical targets alternatively and the difference in velocity between them is calculated. In the case of the heterodyne displacement meter, the sensor is a differential measurement type and the difference in displacement between the two optical targets is detected. The resolution of the measurement of magnetostriction is about 3×10^{-9} for both sensors.

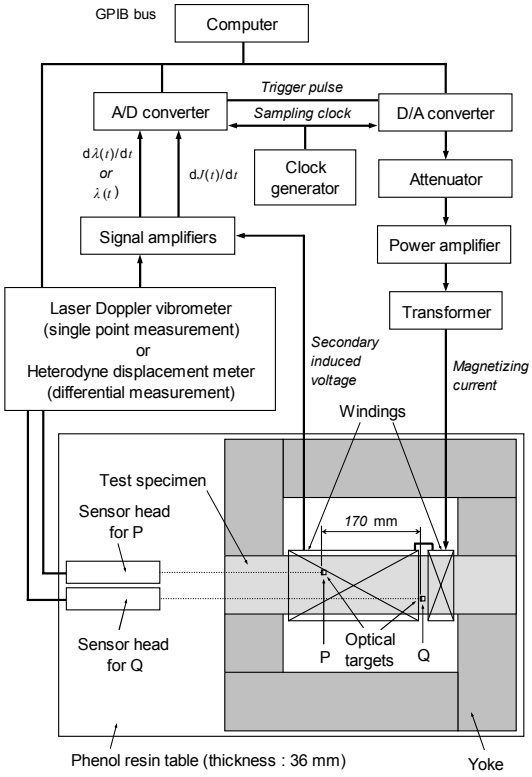

Figure 9a – Measurement system

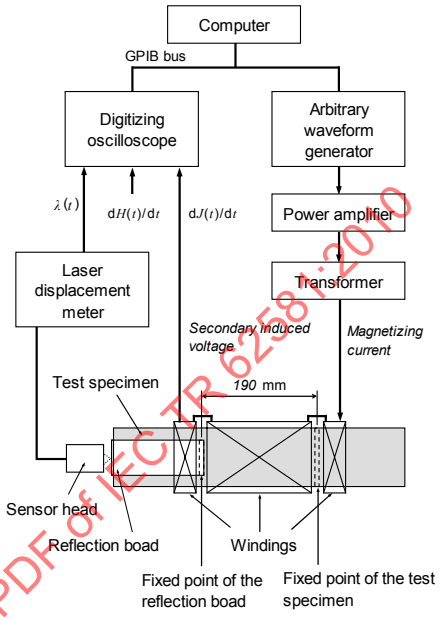

Figure 10a – Measurement system

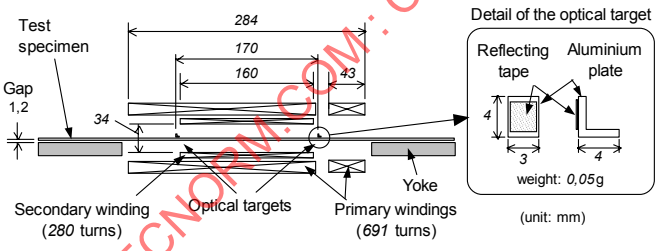

Figure 9b – Section of the test frame

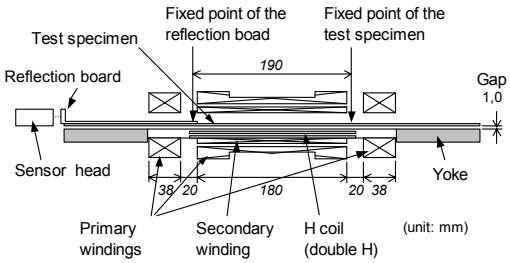

Figure 10b – Section of the test frame

Figure 9 – Measurement system using a laser Doppler vibrometer; differential measurement [4],[5]

Figure 10 – Measurement system using a laser displacement meter; single point measurement [7]

A laser displacement meter using the triangulation method may be used to detect the magnetostriction roughly. Figure 10 shows a measurement system using a laser displacement meter [7]. The test specimen has a length of 500 mm and a width of 100 mm. A closed magnetic circuit is formed using a yoke. The test specimen is fixed to the base plate at one end of the uniform area of magnetic polarization. A reflection board is installed at the other end. The distance between the fixed part of the test specimen and the fixed part of the reflection board is 190 mm. The resolution of the laser displacement meter is 10 nm and the resolution of magnetostriction is $5{,}3 \times 10^{-8}$.

Figure 11 shows a measurement system using a laser displacement meter to detect magnetostriction [6]. The test specimen has a length of 500 mm and a width of 100 mm. A closed magnetic circuit is formed using a vertical double yoke. The vertical orientation of the windings and the test specimen is to avoid mechanical contact of the test specimen with any solid part of the system except the clamp. The test specimen is clamped to the base at the upper end. The magnetized length is 470 mm. A fine grating of a laser linear encoder is attached on the lower part of the test specimen below the yokes. The lower end of the test specimen is connected to the jaws of a hydraulic system. The laser linear encoder measures the displacement of the fine grating, detecting the interference of reflected-diffracted light of a laser source. It has a maximum resolution of 10 nm with 10 kHz periodicity. The resolution of magnetostriction is $1{,}5 \times 10^{-8}$. This system measures the magnetostriction at magnetizing frequencies in the range of 0,5 Hz to 500 Hz.

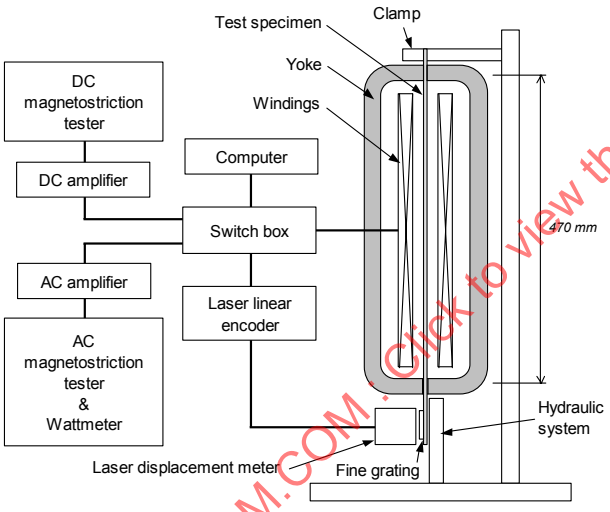

Figure 11 – Measurement system using a laser displacement meter; single point measurement [6]

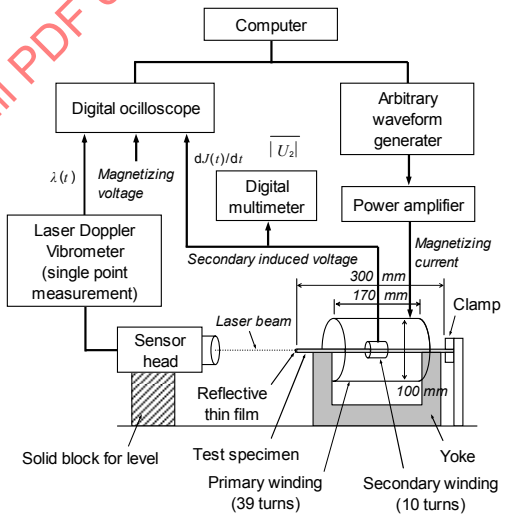

Figure 12 – Measurement system using a laser Doppler vibrometer; single point measurement [8]

A single point laser Doppler vibrometer is used to detect the magnetostriction velocity. Figure 12 shows a measurement system using a single point laser Doppler vibrometer [8]. The test specimen has a length of 303 mm and a width of 30 mm. A closed magnetic circuit is formed using a vertical single yoke. The test specimen is clamped at one end and the laser beam is focused on the other end. The distance between the clamp and the laser focus is 300 mm. The resolution of magnetostriction is $6{,}5 \times 10^{-9}$. This system measures the magnetostriction at magnetizing frequencies in the range of 500 Hz to 3000 Hz.

As shown above, most measurement systems for magnetostriction adopt a single sheet tester with single yoke and test specimen size of 100 mm in width and 500 mm in length. Single yokes are advantageous rather than double type yokes to fix the optical target on the test specimen within the yoke. Horizontal type yokes are more advantageous than vertical type yokes to make coplanar pole faces [28], [29]. Digital sampling methods are essentially adapted to the equipments in all of the above systems: signals of magnetostriction and magnetic polarization

are acquired using 2-channel digitizer and the signals data are processed by computer to determine the magnetostriction characteristics.

5.2 Epstein strip tester

The magnetic cores of electrical machines such as transformers are manufactured from laminations of electrical steel. When machines such as these are built, they invariably contain areas of increased stress. These stresses arise from factors such as non-uniform clamping and temperature variations across the core [18]. Of particular interest is the magnetostriction due to its high stress sensitivity and its major influence on the noise emanating from transformer cores [30]. The system described here is based on the use of accelerometer sensors offering a rapid and user-friendly measurement of the harmonics of magnetostriction together with the simultaneous assessment of power loss and permeability under applied stress.

A schematic diagram of the measurement system is shown in Figure 13. A single Epstein test specimen, which has been stress relief annealed to remove stresses imparted to the specimen during preparation, is inserted into a non-conductive, non-magnetic resin former which is enwrapped by the secondary and primary windings. Flux closure is by way of a wound electrical steel yoke. A mutual inductor is connected in series opposition with the main primary and secondary windings in order to compensate for air flux enclosed by the secondary winding [9],[10],[12],[22].

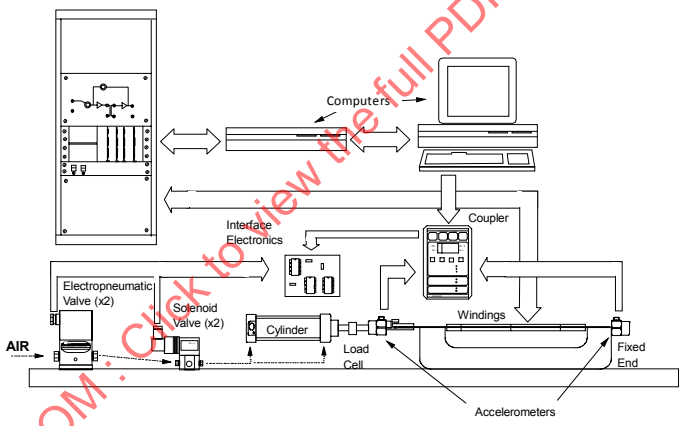

Figure 13 – Schematic diagram of an automated system using accelerometer sensors [12]

The system base also houses the driver electronics which connects to a rack containing the loss tester together with power supplies for the system components. The loss tester generates and controls the magnetization and measures magnetic parameters including power loss, apparent power and permeability. This system is controlled by a dedicated computer, which is itself under the control of the main system computer using RS232 communications. A ROM holding a 2048 increment sinusoid with an 8 bit amplitude resolution is clocked into an analogue to digital converter to give the test waveform [13]. This is then amplified to give the magnetization signal. Negative feedback is taken from the secondary windings via a buffer amplifier to the input of the power amplifier for sinusoidal control of the flux waveform.

Stress is applied uniaxially along the length and in the plane of the 305 mm × 30 mm Epstein test specimen by a low friction, non-rotating cylinder. The pressure in this cylinder is controlled by electro-pneumatic valves which are, in turn, controlled by a d.c. voltage generated by the PC data acquisition card. The computer provides highly controllable stressing by monitoring the output of a lightweight, washer-type in-line load cell utilising a simple control algorithm. Switching between tension and compression is initiated by the computer which uses digital outputs to operate solenoid valves powered by the driver amplifiers. Given a stable pressurised air supply of approximately 0,7 MPa a range of stress values from -10 MPa to 10 MPa can be

applied to the samples under test. It is estimated that the stress in the test specimen can be set with an uncertainty of approximately ± 0,2 MPa.

In this system, the piezoelectric accelerometer was used instead of optical methods. The chosen sensor exhibits a very high sensitivity (1 V/g) together with low mass (< 5 g) and low cross axis sensitivity that makes it ideal for this application. The accelerometer method also eliminates the requirement for accurate, time consuming setting up, as in most of the alternative methods, which is essential for an automated system.

Two accelerometers, containing miniaturised charge amplifiers, are used for the measurement of magnetostriction. The first, mounted on the clamp at the fixed end of the strip, provides a reference signal, whilst the second is incorporated into a clamp attached to the free end of the strip. These accelerometers are connected to a coupler that provides a constant current supply for the sensors and amplifies and filters their output signal. The two channel output from the coupler is summed, as the reference is mounted in the opposite direction to the active sensor and whose output is thus opposite in sign, and passed to the data acquisition card in the main computer. Custom written software then filters, double integrates, calibrates and performs a fast Fourier transform on the data to give the peak value of magnetostriction for several harmonics.

Magnetizing frequencies of 50 Hz or 60 Hz are available although the magnetostriction measurement system is capable of an estimated frequency of 500 Hz for the magnetizing signal, limited by the measurable range of acceleration by the sensors.

The uncertainty in the measurement of magnetostriction is highly dependent on the magnetic and stress states of the test specimen. Taking these influences into consideration it is estimated that the uncertainty in the measurement of magnetostriction is ± 2 %.

The power loss is calculated in the loss tester by firstly evaluating the vector product of the magnetizing field and the flux density derivative using an analogue multiplier. The output of this multiplier is averaged by an amplifier to give a d.c. voltage which is proportional to the power dissipation in the sample. This voltage is digitised by an analogue to digital converter and passed to the computer which calculates the specific total power loss using various scaling factors such as the excitation frequency and sample density. The value of the magnetizing field is assumed to be directly proportional to the magnetizing current passing through a shunt resistor in the ground return of the test frame primary circuit while the secondary voltage is proportional to the derivative of the flux density. At constant temperature, the uncertainty of the specific total loss measurement has been found to be within ± 1 %.

6 Examples of measurement

6.1 Magnetostriction without external stress

Measurements of magnetostriction are usually performed by acquisition of signals of magnetostriction and magnetic polarization by digital sampling methods.

Figure 14 shows an example of magnetostriction characteristics of a high permeability grain-oriented electrical steel sheet 0,30 mm thick for peak magnetic polarizations of 1,3 T; 1,5 T; 1,7 T; 1,8 T and 1,9 T under alternating magnetization of 50 Hz [2]. There are six figures derived from the same data set of signals of magnetostriction and magnetic polarization: (a) signals of magnetostriction, (b) butterfly loops, (c) signals of magnetic polarization, (d) zero-to-peak and peak-to-peak values of magnetostriction versus peak value of magnetic polarization, (e) power spectrum of harmonics in magnetostriction, (f) power spectrum of harmonics in the A-weighted magnetostriction velocity (see Annex C). Vertical axes of (e) and (f) are decibel values referred to 1 μm/m and 1 μm/m/s respectively.

6.2 Magnetostriction under applied stress

Remarkable increases of magnetostriction under applied stress are well known, not only for grain-oriented electrical steel sheets, but also for non-oriented electrical steel sheets [9],[15-17],[22],[23].

Figure 15 shows increases of magnetostriction by compressive stresses in the rolling direction for two grades of grain-oriented electrical steel sheets 0,30 mm thick at peak values of the magnetic polarizations of 1,5 T; 1,7 T and 1,9 T under alternating magnetization of 50 Hz [2]. Stress sensitivity is smaller for the high permeability grade than for the conventional grade of electrical steel.

The sensitivity increases when the compressive stress becomes larger than a threshold stress. Previous work has shown that the threshold stress varies depending on the coating tension and the temperature of the test specimen [9], [15]- [17].

The relationships between the zero-to-peak magnetostriction and the specific total loss with applied stress measured simultaneously for a sample of high permeability grain-oriented electrical steel magnetized to a peak magnetic polarization of 1,5 T, 50 Hz are shown in Figure 16 [12]. The stress sensitivity of magnetostriction is much larger than that of specific total loss.

The magnetostriction of commercial grain-oriented electrical steel is often characterised by a stress sensitivity curve as illustrated in Figure 16. This shows that tensile stress applied along the rolling direction of the steel when magnetized along the same direction has relatively little effect. Compressive stress also has little influence until a threshold value, in this case around 2,5 MPa, is reached whereupon the magnetostriction rises rapidly to a high level. Various factors influence the shape of the stress sensitivity curve, perhaps the most important of which are the surface coatings applied to the steel during its manufacture [19].

Figure 17 shows a typical stress sensitivity curve of magnetostriction and relative permeability measured at 1,5 T (peak), 50 Hz in the rolling direction of the steel. Parameters of interest when comparing materials are (i) the peak maximum value of magnetostriction under compressive stress (in this case around 6×10^{-6}), (ii) the slope of the rise in magnetostriction under compressive stress (in this case around $1,6 \times 10^{-6}$ /MPa) and (iii) the value of compressive stress when the curve reaches its point of inflection (in this case around -5 MPa).

The relationships between the fundamental, second and third harmonics of magnetostriction and applied stress for the same sample at the peak magnetic polarization of 1,5 T, 50 Hz are shown in Figure 18. Again, these results are typical for the material under purely sinusoidal excitation with the large fundamental characteristic and second and third harmonics displaying a similar characteristic with reduced amplitude [12].

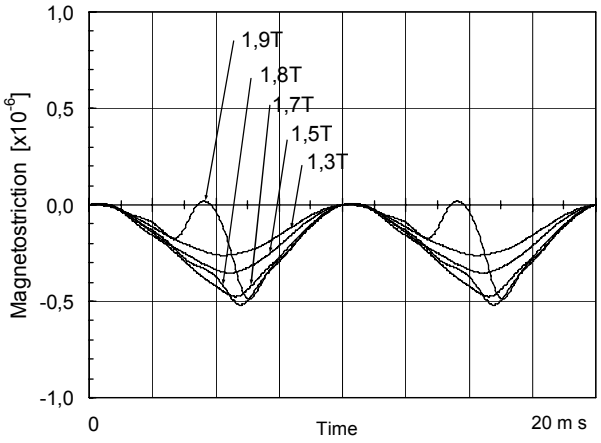

Figure 14a – Magnetostriction curves

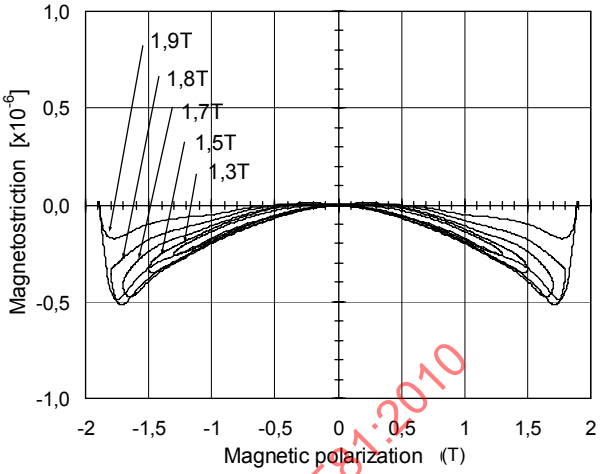

Figure 14b – Butterfly loops

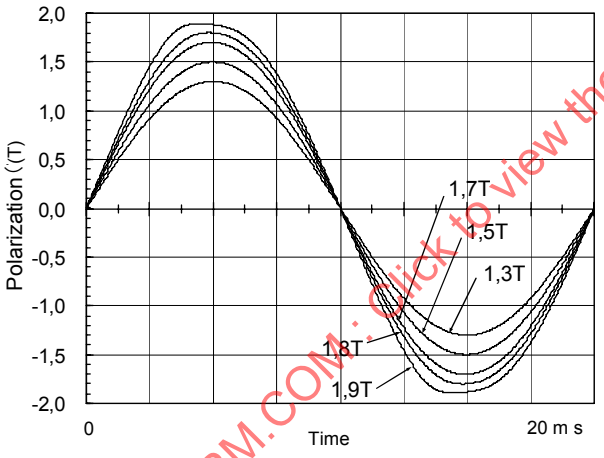

Figure 14c – Magnetic polarization curves

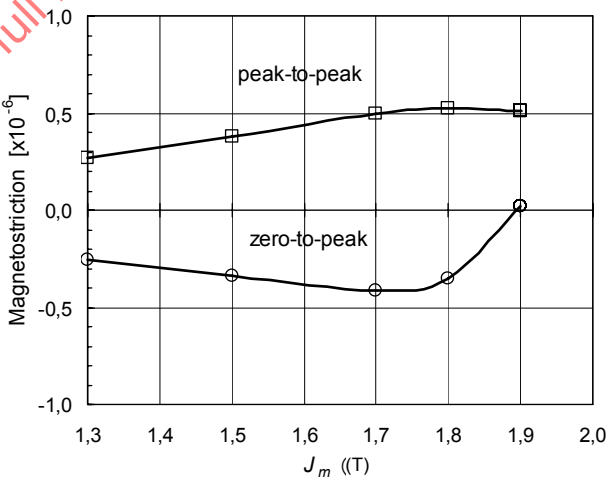

Figure 14d – Zero-to-peak and peak-to-peak values of magnetostriction versus peak value of magnetic polarization

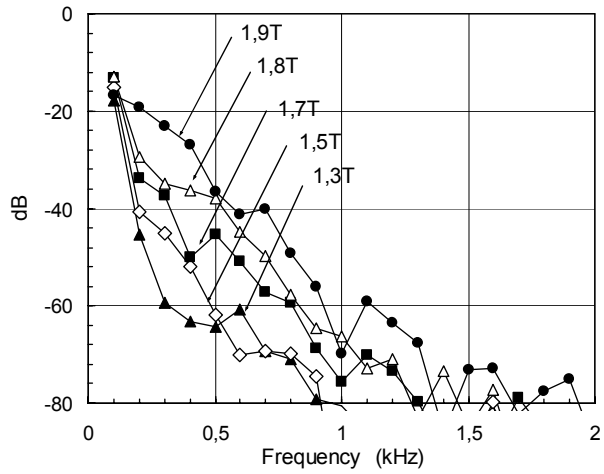

Figure 14e – Power spectrum of harmonics in magnetostriction

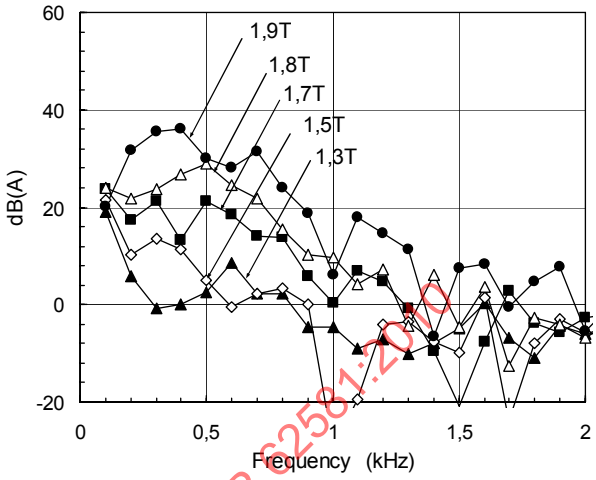

Figure 14f – Power spectrum of harmonics in the A-weighted magnetostriction velocity

Figure 14 – Example of measured results for high permeability grain-oriented electrical steel of 0,3 mm thick sheet; at 1,3 T, 1,5 T, 1,7 T, 1,8 T and 1,9 T, 50 Hz [2]

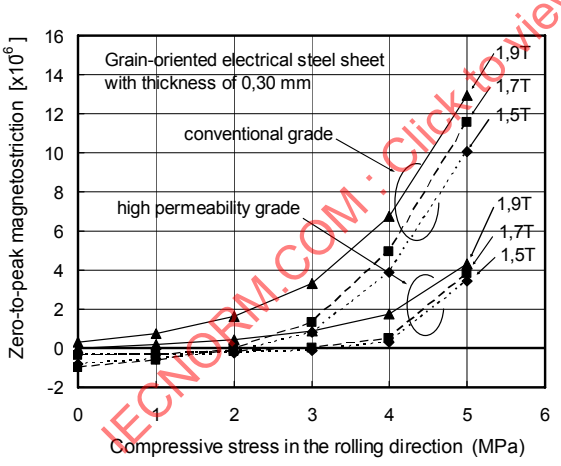

Figure 15 – Increase in magnetostriction with compressive stress in the rolling direction; at 1,5 T, 1,7 T and 1,9 T, 50 Hz [2]

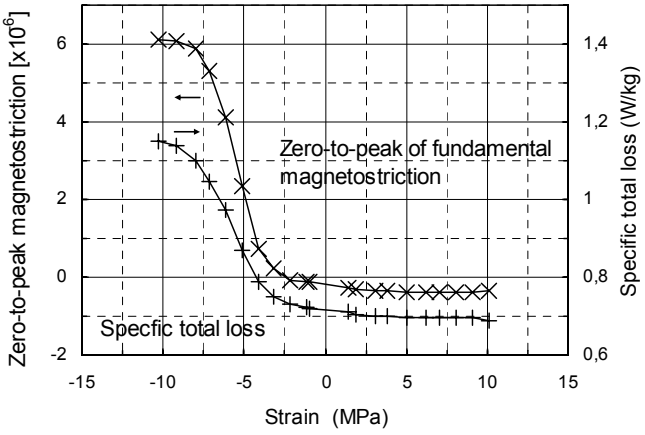

Figure 16 – Typical zero-to-peak magnetostriction versus applied stress for high permeability grain-oriented electrical steel sheet at 1,5 T, 50 Hz [12]

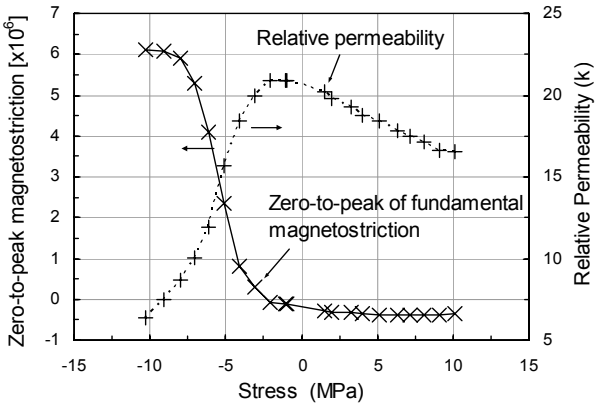

Figure 17 – Stress sensitivity of magnetostriction and permeability in a typical fully processed sample [12]

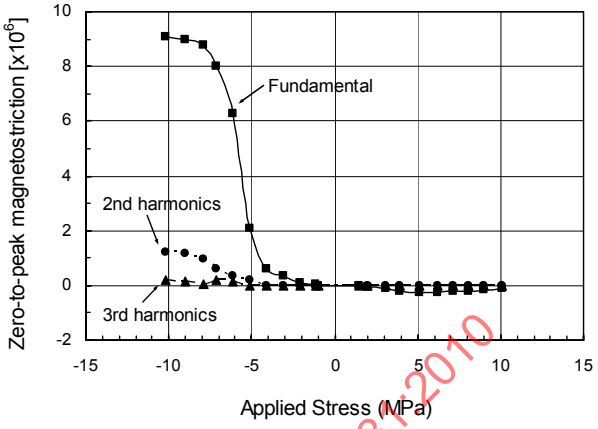

Figure 18 – Typical harmonics of magnetostriction versus applied stress for conventional grain-oriented electrical steel at 1,5 T, 50 Hz [12]

6.3 Variation of magnetostriction with coating tension

Figures 19 and 20 show the variation of maximum magnetostriction under compressive stress at 1,5 T, 50 Hz of around 25 samples each of high permeability and conventional grain-oriented electrical steel with nominal thicknesses from 0,23 mm to 0,30 mm [20].

Figures 21 and 22 show the magnetostriction versus stress characteristic of a typical conventional grain-oriented material at 1,5 T, 50 Hz measured in the rolling direction (RD) and in the transverse direction (TD) respectively. Each point on the curve is the average of four samples from a single batch. The decoated results are taken from the same set of samples with their coatings chemically removed. The main point to note here is the large shift in the curves caused by removal of the coating. In the case of the sample cut in the rolling direction the shift is to the right whereas in the sample cut perpendicular to the rolling direction the shift is to the left. The normal convention is to describe the coating tension as being due to the differential contraction between the coating and the steel substrate. This is illustrated by the shift of the magnetostriction stress curve in the rolling direction on chemical removal of the coating. However, when this model is applied to measurements taken in the transverse to rolling direction, the stress shift is in the compressive direction and would erroneously indicate that the coating holds the steel in compression in the transverse direction. Clearly, this model cannot be applied in the two cases. A model is proposed in Annex B.

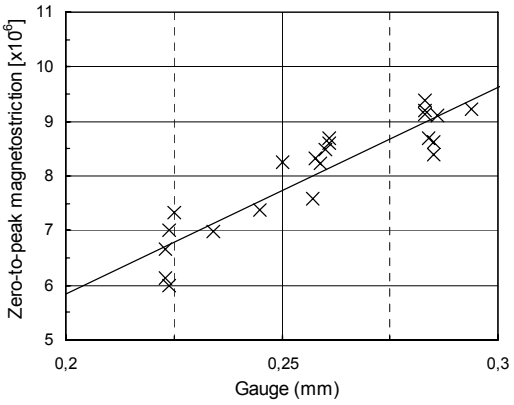

Figure 19 – Variation of maximum magnetostriction under compressive stress in high permeability grain-oriented electrical steel at 1,5 T, 50 Hz [20]

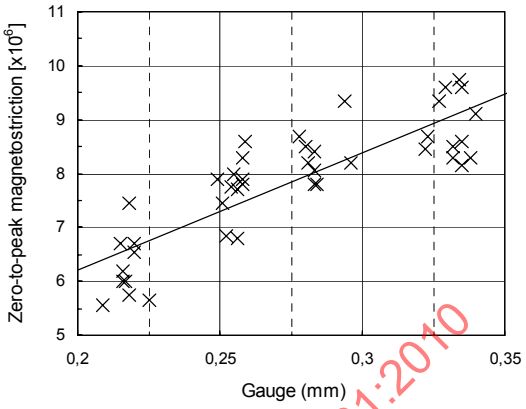

Figure 20 – Variation of maximum magnetostriction under compressive stress in conventional grain-oriented electrical steel at 1,5 T, 50 Hz [20]

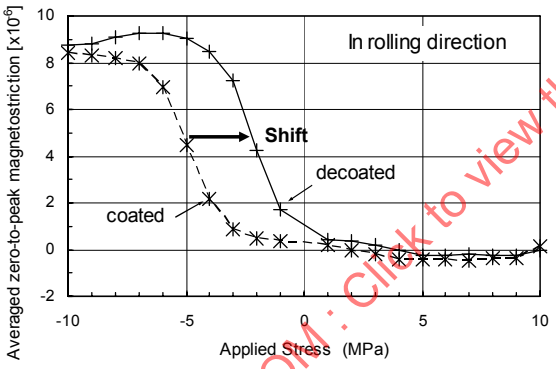

Figure 21 – Magnetostriction versus stress characteristics in the rolling direction of conventional grain-oriented electrical steel before and after coating removal at 1,5 T, 50 Hz [20]

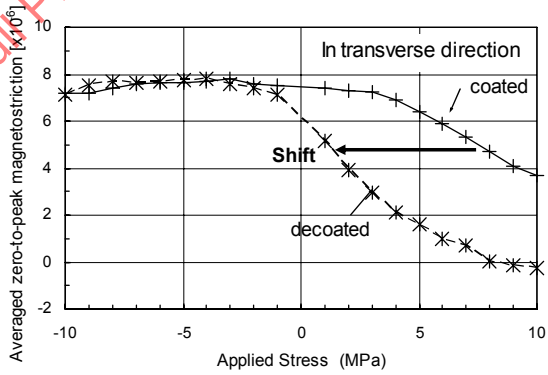

Figure 22 – Magnetostriction versus stress characteristics in the transverse direction of conventional grain-oriented electrical steel before and after coating removal at 1,5 T, 50 Hz [20]

Figures 23 and 24 show the effects of coating tension on the magnetostriction characteristics with the peak values of magnetic polarization for a high permeability grain-oriented electrical steel sheet 0,30 mm thick [17]. Figure 23 shows the cases without external stress and Figure 24 shows the cases under compressive stress of 3 MPa. Three materials with different coating tension are compared at the coating tensions of 3 MPa, 10 MPa and 20 MPa.

Without external stress, the differences between materials with coating tensions of 3 MPa and 10 MPa are clear in the zero-to-peak magnetostriction, but not clear in the peak-to-peak magnetostriction and the A-weighted magnetostriction velocity level below 1,7 T (see Annex C).

However, under an applied stress of 3 MPa, the differences become clear in these magnetostriction characteristics for this range of the peak value of magnetic polarization.

The differences in these magnetostriction characteristics are not clear between coating tensions of 10 MPa and 20 MPa without external stress. Under applied stress of 3 MPa, the differences in the zero-to-peak and peak-to-peak values are clear. However, the difference in the A-weighted magnetostriction velocity level is clear at lower magnetization but becomes smaller with increase in the peak value of magnetic polarization.

Considering the possibility of stress introduced at core manufacturing, the magnetostriction characteristics should be measured, not only without external stress but also under a compressive stress of 3 MPa, in order to assess the contribution of magnetostriction to the acoustic noise emission from transformers and other applications of electrical steel.

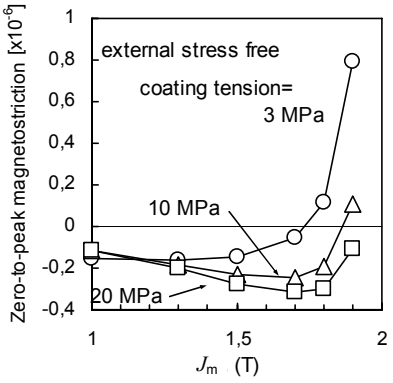

Figure 23a – Zero-to-peak magnetostriction

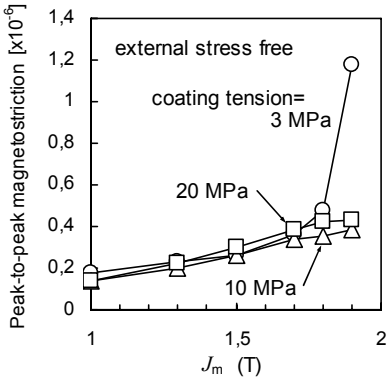

Figure 23b – Peak-to-peak magnetostriction

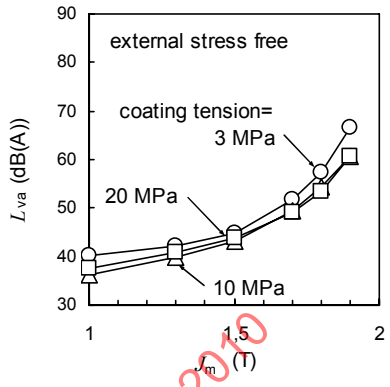

Figure 23c – A-weighted magnetostriction velocity level

Figure 23 – Magnetostriction versus peak value of magnetic polarization for high permeability 0,30 mm grain-oriented electrical steel sheets with three different coatings; external stress was not applied [17]

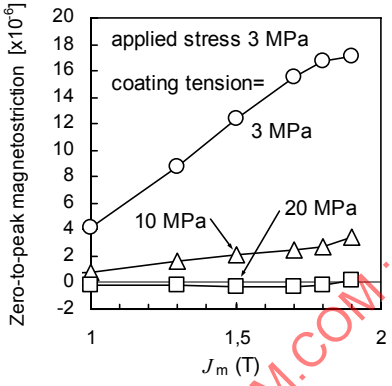

Figure 24a – Zero-to-peak magnetostriction

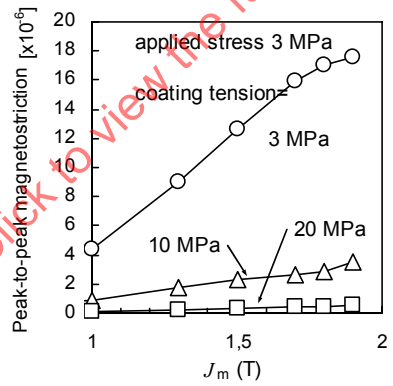

Figure 24b – Peak-to-peak magnetostriction

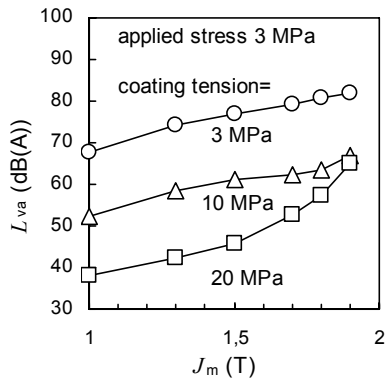

Figure 24c – A-weighted magnetostriction velocity level

Figure 24 – Magnetostriction versus peak value of magnetic polarization for high permeability 0,30 mm grain-oriented electrical steel sheets with three different coatings; external compressive stress of 3 MPa was applied in the rolling direction [17]

In the experience of some steel producers, the external uniaxial tension is twice as effective as the coating tension for iron loss changes in high permeability grain-oriented electrical steel. The coating tension applies stresses not only in the rolling direction but also in the transverse direction. Therefore, the expression of coating stress is dependent on the method of assessment of stress. In this case, the coating tension would be twice the level of coating tension derived from the translation of the magnetostriction – stress curve between the coated and de-coated states.

6.4 Factors affecting precision and reproducibility

6.4.1 General

Various factors affecting the accuracy and reproducibility were examined experimentally using a test specimen of grain-oriented electrical steel sheet, 500 mm in length, 100 mm in width, 0,23 mm in thickness [4], [5].

6.4.2 Overlap length between test specimen and yoke

If the overlap length between the test specimen and the yoke is decreased, the electromagnetic force between the test specimen and the yoke is increased because the flux density in the overlap region is increased. Figure 25 shows the effect of the overlap length on reproducibility of magnetostriction measurement. The reproducibility becomes worse when the overlap length is decreased.

The overlap length should be longer than 25 mm.

6.4.3 The averaging effect on environmental noise

The output of optical sensors may contain an error caused by the environmental noise and it appears even if there is no applied magnetic field. The error can be reduced effectively by averaging the magnetostriction signal for numerous periods of magnetization. Figure 26 shows effects of the averaging number on reduction of the error caused by the environmental noise for two types of optical sensors: a laser Doppler vibrometer and a heterodyne displacement meter [5]. The error decreases hyperbolically with increases in the averaging number. However, a larger averaging number requires a longer measuring time: the averaging number should be selected taking into consideration the reduction of noise and the time for the averaging.

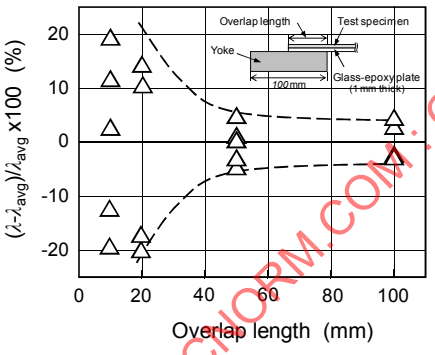

Figure 25 – Effects of overlap length on the reproducibility of measurement [4]

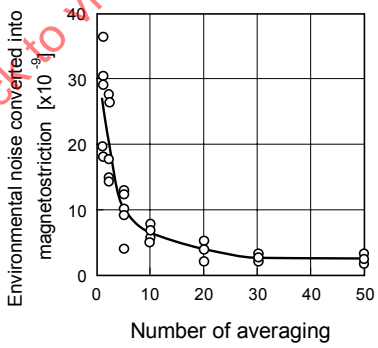

Figure 26a – Laser Doppler vibrometer

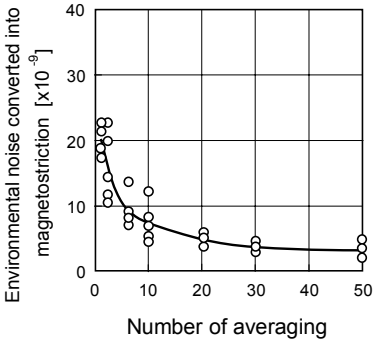

Figure 26b – Heterodyne displacement

Figure 26 – Effect of averaging number on reduction of the error caused by the environmental noise [5]

6.4.4 Gap between test specimen and yoke

Figure 27 shows the effect of the gap between the test specimen and the yoke on the reproducibility of the peak-to-peak magnetostriction [5]. The gap distance was changed by

inserting a glass-epoxy plate of 1,2 mm thickness. The test specimen was removed and installed again at every measurement.

The amount of scatter for a gap distance of 1,2 mm is smaller than without an artificial gap. In the case of a gap distance of 2,4 mm, which is not in Figure 27, it is larger than the others. Therefore, a small gap makes the flux distribution in the gap uniform and can reduce effects of the electromagnetic force between the test specimen and yoke. A wide gap, however, is not appropriate, because it causes a non-uniform flux distribution in the test specimen.

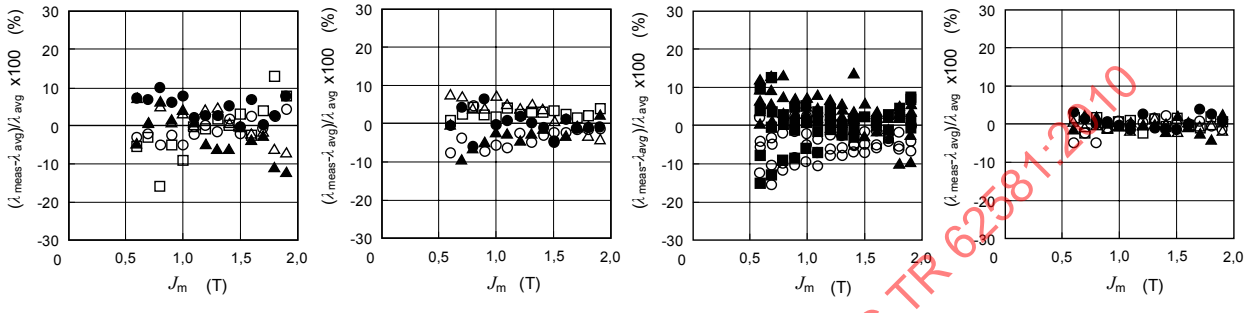

Figure 27a – Without artificial gap

Figure 27b – With gap distance of 1,2 mm

Figure 28a – With reset of the test specimen and the optical targets

Figure 28b – Without reset of the test specimen and the optical targets

Figure 27 – Effect of gap between the test specimen and the yoke on the reproducibility of measurement; the test specimen was reset at every measurement [5]

Figure 28 – Effect of reset of the test specimen on the reproducibility of measurement; the gap distance was 1,2 mm [5]

6.4.5 Resetting the test specimen

The reproducibility is sensitive to the placement of the test specimen in the test frame.

Figure 28a shows the effect of removal and installation of the optical targets and the test specimen on the reproducibility of the peak-to-peak magnetostriction [5]. Fifteen measurements were carried out for the same test specimen. The test specimen was removed and replaced for every measurement. The optical targets were reset every five measurements. The gap distance between the test specimen and the yoke was 1,2 mm. The amount of scatter is within ± 20 %.

The effect of removal and installation of the optical targets can be estimated to be within a few percent from the comparison of Figure 27b and Figure 28a. However, these experiments were examined by the system with two optical targets on the test specimen as shown in Figure 10 and the effect was improved over systems with one optical target on the test specimen.

In order to validate the repeatability of the system, measurements are carried out continuously without reset of the specimen and optical targets. Five measurements were done at each magnetic polarization. Figure 28b shows the scatter of the continuous measurement. The amount of scatter is within ± 5 %.

7 Methods of evaluation of the magnetostriction behaviour

7.1 Relationship between magnetostriction and magnetic domain structure

Magnetostriction is one of the magnetic properties that accompany ferromagnetism. In order to estimate, and improve, magnetostriction behaviour, considerations of the magnetizing processes in magnetic materials are essential.

It is well known from early studies that motions of 180° domain walls do not contribute to the magnetostriction, while changes in 90° domain volumes and rotations of the self-magnetization do have a significant influence on the magnetostriction [15].

Electrical steel sheets are usually comprised of many magnetic domains with differing directions of self-magnetization and each magnetic domain is elongated in the direction of self-magnetization. When an external magnetic field is applied, increases in volume of magnetic domains, where the self-magnetization is along the applied field, occur at first and rotations of the self-magnetization to align with the applied field occur at higher magnetic field strengths. Consequently, the magnetic polarization increases and magnetostriction strain is generated.

Figure 29 shows a magnetic domain pattern on a grain-oriented electrical steel sheet. Wide black and white stripes are 180° domains and the self-magnetization is in opposite directions beyond the domain wall. Narrow triangles in 180° domains, namely lancet domains, are also 180° domains but accompany 90° domains under them. Directions of the self-magnetization in 90° domains are perpendicular to those in 180° domains and trend to the surface. Changes in volume of 90° domains are significant causes of magnetostriction as shown in Figure 30.

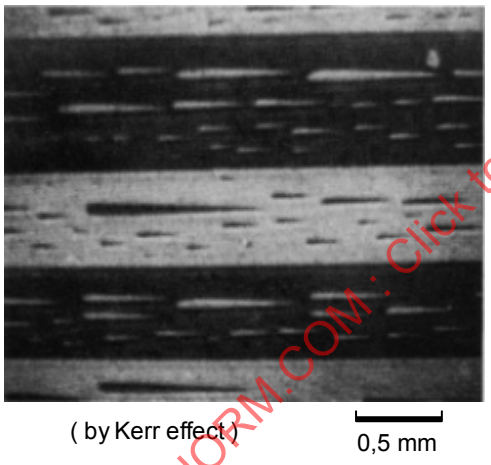

Figure 29 – Magnetic domain patterns on a grain-oriented electrical steel sheet [2]

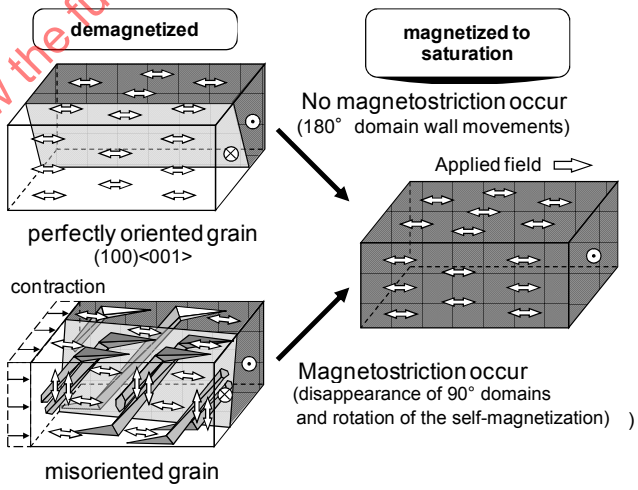

Figure 30 – Schematic diagrams for explanation of magnetic domains and magnetostriction [2],[17]

These 90° domains naturalize magneto-static energy on the surfaces caused by inclines of the self-magnetization to the surfaces. The 180° domain walls also have the function and therefore there are little lancet domains beside 180° domain walls as shown in Figure 28. Therefore increases of width of 180° domain cause increases of volume fraction of 90° domains and decrease of the magnetostriction.

At higher magnetic polarization, after annihilation of main 180° walls, the magnetic polarization increases by suppressions and collapses of 90° domains and causes an increase in magnetostriction.

At higher magnetic field strengths, rotations of the self-magnetization to the applied field arise and cause an increase in magnetostriction.

7.2 A simple model of magnetostriction behaviour

A simple model, describing the polarization dependence of the peak-to-peak and zero-to-peak magnetostriction of grain-oriented electrical steels based on the domain structure behaviour has been proposed [27]. The hysteresis behaviour of the butterfly loop is not considered in this model.

Three main features of the domain structure have been considered in relation to the zero-to-peak magnetization with the increase of polarization:

Part I: at lower polarizations, a slight exponential decrease of the magnetostriction occurs according to the increase of volume fraction of 90° domains owing to the movement of 180° domain width;

Part II: at higher polarizations, a Dirac-type functional increase of the magnetostriction occurs according to the suppression and collapse of 90° domains owing to the annihilation of main 180° domain walls;

Part III: at higher magnetic field strengths, a sharp increase of the magnetostriction occurs owing to the rotation of the self-magnetization to the applied field.

These relationships were formulated for the polarization dependence of the peak-to-peak and zero-to-peak magnetostriction [27]:

$$\lambda_{\mathrm{o-p}}(J_{\mathrm{m}}) = \mathrm{D}\left[e^{(a+\Delta a)(J_{\mathrm{m}}-J_0)} + \frac{e^{a(J_{\mathrm{m}}-J_0)}}{e^{(J_{\mathrm{m}}-J_{\mathrm{c}})/\Delta J}+1}\right] \tag{11}$$

$$\lambda_{\mathrm{p-p}}(J_{\mathrm{m}}) = \mathrm{D}\left[e^{(a+\Delta a)(J_{\mathrm{m}}-J_0)} + \frac{e^{a(J_{\mathrm{m}}-J_0)}}{e^{(J_{\mathrm{m}}-J_{\mathrm{c}})/\Delta J}+1}\right] \tag{12}$$

where

$\lambda_{\mathrm{o-p}}(J_{\mathrm{m}})$ is the zero-to-peak magnetostriction at a peak value of magnetic polarization J_{m} ;

$\lambda_{\mathrm{p-p}}(J_{\mathrm{m}})$ is the peak-to-peak magnetostriction at a peak value of magnetic polarization J_{m} ;

D is a dimensionless coefficient;

a is a parameter to regulate the exponential increment, in per tesla;

Δa is an increase in the value of a between Part I to Part III, in per tesla;

J_{m} is the peak value of magnetic polarization, in tesla;

J_0 is a value near to saturation polarization, in tesla;

J_{c} is the middle value of Dirac-type distribution function, in tesla;

ΔJ is the half-width of Dirac-type distribution function, in tesla.

The actual values of these parameters are determined by a least squares fitting of the measured data as shown in Figure 31. Figure 32 shows a typical comparison between the measured values and the fitted values obtained by equations (11), (12).

The behaviour of 90° domains in Parts II and I are a function of the magnetic polarization and are affected by coating tension and strain. However, the rotation of the self-magnetization to the applied field in Part III is a function of magnetic field strength and depends on texture.

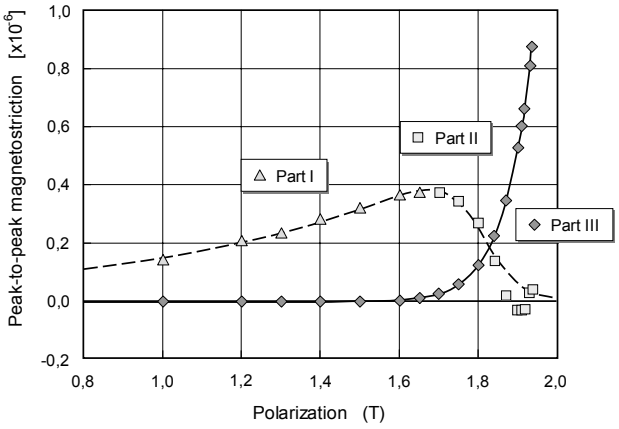

Figure 31 – Separation of the different features of peak-to-peak magnetostriction according to the proposed model [27]

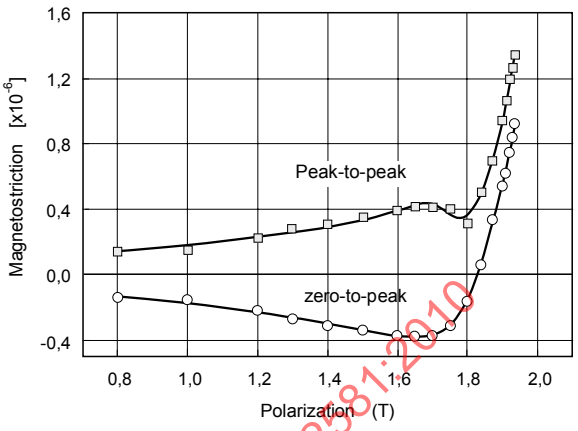

Figure 32 – Measured peak-to-peak and zero-to-peak magnetostriction of a grain-oriented electrical steel sheet with fitted curves according to the proposed model [27]

Figure 33 shows the effects of coating tension on the magnetostriction of a grain-oriented electrical steel sheet [17] where, λ_{sp} is a normalized value of zero-to-peak magnetostriction to the value at saturation polarization. The value λ_{sp} is negative, in principle, and the lower values of λ_{sp} indicate the larger volume of 90° domain. At lower magnetic polarizations, the lower coating tension causes the larger volume of 90° domains to occur. However, the coating tension almost does not change the behaviour of magnetostriction near saturation polarization corresponding to part III.

In contrast, Figure 34 shows the effect of strain introduced by laser irradiation [17]. In the demagnetized state, the higher energy density of laser irradiation causes a larger volume of 90° domains. However, the behaviour of λ_{sp} at higher magnetic polarizations is different from that in Figure 33. This model can explain this behaviour. It is considered that the volume of 90° domains introduced by laser irradiations is almost independent of the 180° domain width and then the behaviour of magnetostriction corresponding to Part I does not appear at the higher energy density of laser irradiation. The behaviour of magnetostriction corresponding to Parts II and III may not be changed by the laser irradiation.

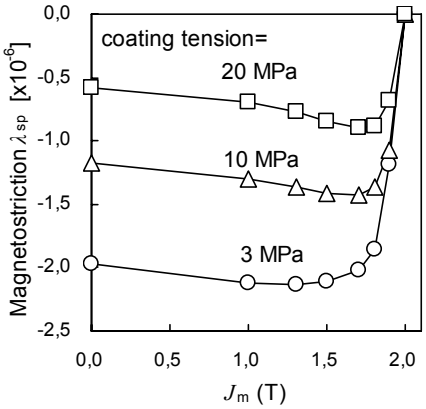

Figure 33 – Effect of coating tension on $J_m - \lambda_{sp}$ curves; λ_{sp} is the normalized value of zero-to-peak magnetostriction to the value at saturation polarization [17]

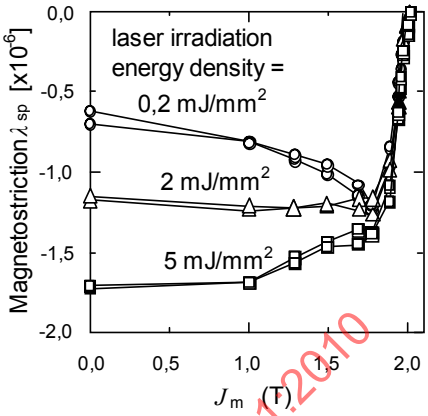

Figure 34 – Effect of laser irradiation on $J_m - \lambda_{sp}$ curves; λ_{sp} is the normalized value of zero-to-peak magnetostriction to the value at saturation polarization [17]

Annex A
(informative)

Requirements concerning the prevention of out-of-plane deformations

The largest obstacle to the measurement of magnetostriction is the occurrence of out-of-plane deformations of the test specimen during the measurement. In an alternating magnetic field, it becomes out-of-plane vibrations. If the test specimen is kept plane with or without an applied field, there is no out-of-plane deformation. The causes of the out-of-plane deformation are considered as followed:

– waviness of the test specimen;

– uneven surfaces of the supports for the test specimen;

– resonance of the test specimen.

In order to estimate the influence of the out-of-plane deformation, a bending of sheet with a length of 500 mm is considered as shown in Figure A.1. Figure A.2 shows the relationship between the change of distance between both ends of the sheet $\Delta l / l_{\mathrm{m}}$ and the distance of out-of-plane deformation d .

In order to satisfy a resolution for magnetostriction of 1×10^{-8}, the magnitude of the out-of-plane deformation must be less than 30 μm.

The means to prevent the out-of-plane deformation are as follows:

– use a flat test specimen without any transformation;

– keep a coplanar surface under the test specimen: the pole faces, inner bottom of the winding form, the under plate of clamp and the filling plates between the winding form and pole faces;

– place a thin glass or a light load on the test specimen.

When the out-of-plane deformation occurs, a phase shift between signals of the magnetic polarization and the magnetostriction occurs and then the butterfly loop is transformed. Observations of the butterfly loop during the measurement are necessary [8].

The resonance frequencies of grain-oriented electrical steel sheets are reported:

– 5150 Hz for 387 mm long by 100 mm wide by 0,14 mm and 0,35 mm thick [3];

– 4500 Hz for 300 mm long by 30 mm wide by 0,27 mm thick [8].

Therefore the frequency used for the measurement of magnetostriction of grain-oriented electrical steel sheet should be below 1 kHz.

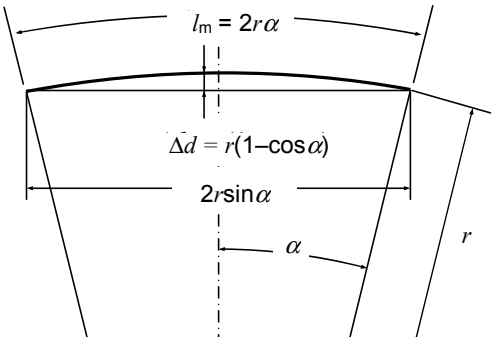

Figure A.1 – Schematic diagram of out-of-plane deformation of test specimen (length l_m) with radius r

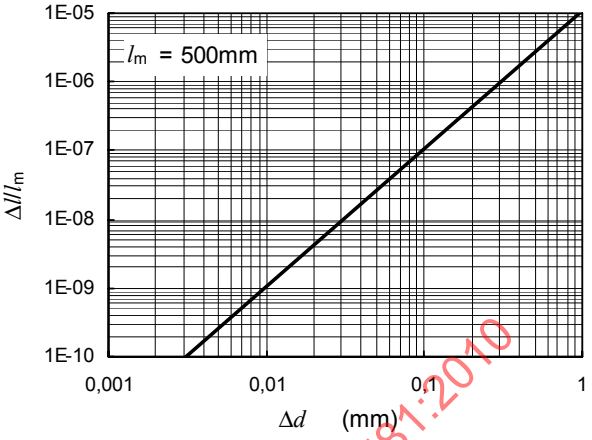

Figure A.2 – Errors in length change of the test specimen $\Delta l / l_m$ versus out-of-plane deformation distance Δd